



Published in final edited form as:

Sci Total Environ. 2014 July 15; 487: 173–186. doi:10.1016/j.scitotenv.2014.03.131.

PAHs (Polycyclic Aromatic Hydrocarbons), Nitro-PAHs, Hopanes and Steranes Biomarkers in Sediments of Southern Lake Michigan, USA

Lei Huang, Sergei M. Chernyak, and Stuart A. Batterman*

Department of Environmental Health Sciences, University of Michigan, Ann Arbor, MI, USA

Abstract

PAHs in the Great Lakes basin are of concern due to their toxicity and persistence in bottom sediments. Their nitro derivatives, nitro-PAHs (NPAHs), which can have stronger carcinogenic and mutagenic activity than parent PAHs, may follow similar transport routes and also are accumulated in sediments. Limited information exists regarding the current distribution, trends and loadings of these compounds, especially NPAHs, in Lake Michigan sediments. This study characterizes PAHs, NPAHs, and biomarkers steranes and hopanes in surface sediments collected at 24 offshore sites in southern Lake Michigan. The ΣPAH_{14} (sum of 14 compounds) ranged from 213 to 1291 ng/g dry weight (dw) across the sites, levels that are 2 to 10 times lower than those reported 20 to 30 years earlier. Compared to consensus-based sediment quality guidelines, PAH concentrations suggest very low risk to benthic organisms. The ΣNPAH_5 concentration ranged from 2.9 to 18.6 ng/g dw, and included carcinogenic compounds 1-nitropyrene and 6-nitrochrysene. $\Sigma\text{Sterane}_6$ and ΣHopane_5 concentrations ranged from 6.2 to 36 and 98 to 355 ng/g dw, respectively. Based on these concentrations, Lake Michigan is approximately receiving 11, 0.16, 0.25 and 3.6 metric tons per year (t/yr) of ΣPAH_{14} , ΣNPAH_5 , $\Sigma\text{Sterane}_6$ and ΣHopane_5 , respectively. Maps of OC-adjusted concentrations display that concentrations decline with increasing off-shore distance. The major sources of PAHs and NPAHs are pyrogenic in nature, based on diagnostic ratios. Using chemical mass balance models, sources were apportioned to emissions from diesel engines (56±18%), coal power plants (27±14%), coal-tar pavement sealants (16±11%), and coke ovens (7±12%). The biomarkers identify a combination of petrogenic and biogenic sources, with the southern end of the lake more impacted by petroleum. This first report of NPAHs levels in sediments of Lake Michigan reveals several carcinogenic compounds at modest concentrations, and a need for further work to assess potential risks to aquatic organisms.

© 2014 Elsevier B.V. All rights reserved.

*Corresponding author: Stuart Batterman, Ph.D., Professor, Environmental Health Sciences, School of Public Health, University of Michigan, Civil and Environmental Engineering, College of Engineering, University of Michigan, M6075 SPH II, 1415 Washington Heights, Ann Arbor, Michigan 48109-2029, Office: (734) 763-2417; Fax: (734) 936-7283, stuartb@umich.edu.

Conflict of interest

No conflict of interest to be declared.

Publisher's Disclaimer: This is a PDF file of an unedited manuscript that has been accepted for publication. As a service to our customers we are providing this early version of the manuscript. The manuscript will undergo copyediting, typesetting, and review of the resulting proof before it is published in its final citable form. Please note that during the production process errors may be discovered which could affect the content, and all legal disclaimers that apply to the journal pertain.

Keywords

Polycyclic aromatic hydrocarbons (PAHs); nitro-PAHs (NPAHs); hopanes; steranes; sediment; Great Lakes

1. Introduction

Polycyclic aromatic hydrocarbons (PAHs) are a group of widely distributed and persistent organic pollutants that include a number of carcinogenic compounds (ATSDR, 1995). There are three major types of PAH sources: pyrogenic PAHs that are emitted during incomplete burning of coal, oil, gas, coke, wood, garbage, or other organic material; petrogenic PAHs that form in the earth by geological processes at low temperature, possibly high pressure and over long time periods that are the basis for crude oil, coal, coal tar pitch, and asphalts; and diagenetic PAHs that are derived from biogenic precursors like plant terpenes and in sediments (Crane et al., 2010). Most PAHs are pyrogenic in origin and are released into the atmosphere (Baek et al., 1991; Neff, 1979). Inputs to aquatic environments arise from atmospheric deposition, urban stormwater runoff and municipal/industrial effluents (Helfrich and Armstrong, 1986). Petroleum spills may be a significant PAH source in certain locations (Helfrich and Armstrong, 1986). Recently, coal-tar pavement sealants have been identified as an important source of PAHs in urban waterways, especially in central and eastern U.S. (Van Metre and Mahler, 2010). Sealed pavements also emit PAHs by volatilization to urban air (Van Metre et al., 2012).

The presence of PAHs in the Great Lakes has been of concern for decades (EPA, 1994; EPA, 2000; EPA&EC, 2004; Sun et al., 2006a; Sun et al., 2006b). The Lakes' large surface areas increase atmospheric deposition (Simcik et al., 1999), and the long hydrologic retention times and great depths increase their sensitivity to inputs (De Vault et al., 1996). Lake Michigan receives large inputs of PAHs from atmospheric deposition, urban runoff and municipal/industrial effluents due to the large urban and industrial centers that surround its southern portion (Helfrich and Armstrong, 1986). The Lake also receives inputs from petroleum spills given that Indiana Harbor, Indiana and Chicago, Illinois are major distribution centers for petroleum products (Helfrich and Armstrong, 1986). In 1980, the cumulative loadings of PAH from these sources was estimated to be 50 to 55 metric tons/year (MT/yr), which included 40 MT/yr from atmospheric deposition (based on measured ΣPAH_{12} concentrations in air and dry and wet deposition rates) (Andren and Strand, 1979), 0.8 to 8 MT/yr from urban runoff/municipal effluent (based on measured ΣPAH_{22} concentrations in sewage discharge and combined runoff/effluent flows) (Kveseth et al., 1982), and 5 to 7.5 MT/yr from commercial and private vessels and petroleum spills (Helfrich and Armstrong, 1986). PAHs in Lake Michigan sediments have been characterized in several major studies conducted in the 1980s and 1990s (Eadie et al., 1982; Helfrich and Armstrong, 1986; Simcik et al., 1996). Surface sediment accumulation rates for ΣPAH_{17} were estimated to be 50–70 ng/cm²-yr in 1991–1993 (Simcik et al., 1996). While recent declines in PAH levels have been observed in sediment cores from Grand Traverse Bay, Lake Michigan (Schneider et al., 2001), only two studies (Eadie et al., 1982; Helfrich and Armstrong, 1986) have reported PAH levels in sediments in the Lake's southern basin, the

area closest to the source areas around Chicago, Illinois and Gary, Indiana where levels are likely to be highest. Several studies have examined sediments in Areas of Concern (AOC) of southern Lake Michigan, including Grand Calumet, Waukegan Harbor, Milwaukee Estuary, and Muskegon Lake (Ghosh et al., 2003; Kannan et al., 2001; Kemble et al., 2000; Li et al., 2003; MacDonald et al., 2002). The National Coastal Condition Assessment (NCCA) project is planning to analyze near-shore sediments from the Great Lakes for 25 PAHs (EPA, 2010). However, studies on open water sediments have not been carried out since the 1980s. Thus, assessment of current PAH levels in open lake sediments is needed to understand contaminant trends and the potential for environmental risks.

Nitro-PAHs (NPAHs), which are nitrated PAHs, have diverse properties like their parent PAH compounds. As derivatives of PAHs, NPAHs have been found in similar environmental compartments as PAHs (Ozaki et al., 2010; Perrini et al., 2005). They result from direct emissions from combustion sources as well as atmospheric transformations of PAHs (Perrini et al., 2005; Yaffe et al., 2001). Airborne NPAHs also can enter aquatic environments through atmospheric deposition and urban runoff (Ozaki et al., 2010). Although concentrations are far lower than levels of parent PAHs (Albinet et al., 2007; Khalek et al., 2011; Ozaki et al., 2010), NPAHs can have stronger carcinogenic and mutagenic activity (Schantz et al., 2001). Several NPAHs are direct-acting mutagens, e.g., dinitropyrene in diesel particulate matter (Perrini et al., 2005). Although the behavior of NPAHs in the atmosphere has been extensively studied (Albinet et al., 2007; de Castro Vasconcellos et al., 2008; Hayakawa et al., 2002; Librando and Fazzino, 1993), few studies have investigated the occurrence of NPAHs in aquatic environments. The Minnesota Pollution Control Agency (MPCA) measured PAHs and NPAHs in urban stormwater pond sediments (Crane et al., 2010). While NPAHs were not detected in pond stations in the Twin Cities, MN, metropolitan area (Crane, 2014), NPAHs including 2-nitrofluorene, 1-nitropyrene and 6-nitrochrysene were detected at ppb to ppm levels in Varney Pond, White Bear Lake, MN (MDH, 2011). In Europe, NPAHs including nitronaphthalenes, 9-nitronaphthalene, 1-nitropyrene, 6-nitrochrysene and dinitropyrenes have been found at ppb levels in sediments from the Elbe River basin, Germany and Czech Republic (Lübcke-von Varel et al., 2012; Lubcke-von Varel et al., 2011). In sediments of the Suimon River, Japan, 1-nitropyrene and 2-nitrofluorene were measured at ppb levels (Sato et al., 1985). In marine (coastal) sediments collected off Barcelona, Spain, 1-nitropyrene and 6-nitrochrysene were found to contribute to the mutagenic activity (Fernandez et al., 1992), and NPAHs in the Hiroshima Bay Area, Japan, were found at concentrations up to 30 ng/g (2-nitrofluoranthene) (Ozaki et al., 2010). No information has been located regarding NPAHs in Great Lakes sediments.

Hopanes and steranes are two additional classes of semivolatile organic compounds (SVOCs). These compounds are derived from the cell membranes of prokaryotes (Ourisson and Rohmer, 1992; Ourisson et al., 1987) and eukaryotes (Mackenzie et al., 1982), respectively, and are common constituents of crude oil (Manan et al., 2011). Petrogenic (crude oil and derived products) and biogenic sources (vascular plants, algae, bacteria) tend to have distinct hopane and sterane profiles (Bieger et al., 1996). As examples, $\beta\beta$ -hopane configuration is biogenic; $\alpha\beta$ -hopane configuration is thermodynamically stable and dominates in petroleum; the mono-unsaturated hopanes (e.g., C30-hopenes) are also

biogenic; and there are indicators of thermal maturity that utilize the ratios between isomers or diastereomers (Boitsov et al., 2011; Qu et al., 2007). Because these compounds are resistant to chemical, photochemical and microbial degradation (Manan et al., 2011; Neff and Durell, 2012), hopanes and steranes have been used as signature or marker compounds to help identify sources of organic matter in lake sediments (Meyers and Ishiwatari, 1993; Qu et al., 2007; Xiong et al., 2010), the extent of biodegradation (Prince et al., 1994), and as tracers of vehicle exhaust in the atmosphere (given their specificity to lubricating oils used in diesel and gasoline engines) (Kleeman et al., 2007; Schauer et al., 1999; Schauer et al., 2002). Information regarding hopanes and steranes in the Great Lakes is scarce. These compounds were detected in western Lake Ontario sediments where direct input of crude oil or petroleum products was indicated (Kruge et al., 1998). Hopanes and steranes were also used to identify the source of the 2009 Sarnia oil spill in Lake Huron (Wang et al., 2011b). However, these compounds have not reported for Lake Michigan.

The objective of this paper is to characterize PAHs, NPAHs, hopanes and steranes in surficial sediments from the southern basin of Lake Michigan. The analysis includes an evaluation of compositional profiles, spatial patterns and loadings. Semi-quantitative forensic techniques (diagnostic ratios) are used to identify sources of target compounds, and quantitative CMB modeling is used to apportion PAH sources. Temporal trends of PAHs are derived in conjunction with literature data. This first report regarding NPAHs and biomarkers in sediments of Lake Michigan provides information that can be used to monitor trends over time, identify sources of hydrocarbon contamination, and evaluate health and ecological consequences.

2. Materials and methods

2.1 Sample collection

Sediment samples were collected as “add-ons” to an ongoing program designed to assess long term trends in benthic communities in southern Lake Michigan, which has been conducted by the National Oceanic and Atmospheric Administration (NOAA) Great Lakes Environmental Research Laboratory (GLERL) at the same 40 sites since 1980. Of these, we selected 24 offshore sites (Figure 1) intended to sample various locations, depths and sediment types across the southern basin of Lake Michigan. Most sites (except S-2, S-3, S-4, V-1, H-8, B-7) were in depositional zones (Corcoran, 2013). Sampling took place from August 16 to 19, 2011 on the R/V Laurentian (NOAA GLERL) using EPA methods (USEPA, 1999). The top 1 cm of sediment was collected by a Ponar Dredge, placed in solvent-washed brown glass jars with PTFE (polytetrafluoroethylene)-lined screw caps, and stored at 4 °C in a refrigerator on board. Immediately after the expedition, samples were transported in coolers to our Ann Arbor, Michigan laboratory and stored at -20 °C for two weeks before extraction.

2.2 Materials

All solvents were HPLC grade and obtained from Fisher Scientific Inc. (Pittsburgh, PA, USA). Florisil (60–100 mesh) and sodium sulfate (anhydrous, certified ACS granular, 10–60 mesh) for column chromatography were supplied by the same vendor. The target

compounds included 16 PAHs, 11 NPAHs, 5 hopanes and 6 steranes, (Table 1). PAHs included the 16 EPA priority PAHs (CFR, 1982). The target NPAHs were selected since they have been frequently detected in airborne and diesel exhaust PM samples (Bamford and Baker, 2003; Huang et al., 2013; Khalek et al., 2011; Liu et al., 2010; Reisen and Arey, 2005). The target hopanes and steranes are those most frequently found at relatively high concentrations in sediments and diesel exhaust PM samples (Boitsov et al., 2011; Khalek et al., 2011; Liu et al., 2010; Qu et al., 2007; Schauer et al., 1999; Schauer et al., 2002).

Authentic standards of PAHs, NPAHs and biomarkers were purchased from Cambridge Isotope Laboratories (Andover, MA), Sigma-Aldrich, (St. Louis, MO), and Chiron AS (Trondheim, Norway), respectively. Internal standards (ISs) for PAHs were fluoranthene-d10 (Cambridge Isotope Laboratories Inc., Andover, MA, USA) and an IS PAH mixture (Wellington Laboratories, Guelph, ON, Canada). 1-Nitrofluoranthene-d9 (Cambridge Isotope Laboratories Inc., Andover, MA, USA) was used as an IS for NPAH analyses, and n-tetracosane-d50 (Chiron Laboratories, Trondheim, Norway) as an IS for hopanes and steranes. Surrogate standards included C27- α,α,α -(20R)-cholestane-d2, 1-nitropyrene-d9, chrysene-d12 and naphthalene-d8 (Chiron Laboratories, Trondheim, Norway).

2.3 Sample preparation and chemical analysis

After decanting the water layer on top of each sediment sample and homogenization, a 10-g subsample was taken to which 15 μ L of the surrogate standard was added. The sample was dried with Na_2SO_4 , extracted twice using dichloromethane/hexane (4:1, v/v), sonicated for 30 min, and any remaining solids were separated by centrifugation and removed. Extracts were passed through an activated Florisil column and fractionated into three portions using different solvents: fraction A was eluted with 15 mL of hexane; fraction B with 15 mL of hexane/acetone (1:1, v/v); and fraction C with 30 mL of methanol. Each fraction was evaporated under a nitrogen stream to 1 mL volume, transferred to a storage vial with a Teflon crimp seal, and stored at 4 °C until analysis. Fractions A, B and C were analyzed for hopanes and steranes, PAHs, and NPAHs, respectively.

Target compounds were quantified using a gas chromatograph-mass spectrometer (GC-MS; HP 6890/5973, Agilent Industries, Palo Alto, CA, USA), an autosampler, and splitless 2 μ L injections. Injector and detector temperatures were 275 °C and 280 °C, respectively. Separations used a capillary column (DB-5, 30 m \times 0.25 mm id; film thickness 0.25 μ m; J&W Scientific, Folsom, CA, USA). The carrier gas was helium (1.5 mL/min, pressure of 37.4 kPa, average velocity of 31 cm/s), and the MS reagent gas was ultra-high purity methane. Details of the temperature programs and other instrumental parameters have been described previously (Huang et al., 2013). The MS detector was operated in electron impact (EI) mode for PAHs, hopanes and steranes, and in negative chemical ionization (NCI) mode for NPAHs. All analytes were individually quantified against authentic standards. In each case, 15 μ L of the IS was added to each sample extract using a 25 μ L syringe prior to GC/MS analysis.

Quality assurance (QA) measures included the regular use of field and lab blanks, replicates, surrogate spike recovery tests and standard reference material (SRM 2266, NIST, USA). Replicates were performed for six samples (i.e., one replicate for every 4 samples).

Measurement precisions, expressed as the average relative percent difference (RPD) across the six replicate measures and compounds in the group, were 22%, 19%, 26% and 23% for PAH, NPAH, sterane and hopanes determinations above the reporting limits, respectively. Several target compounds were detected, but at trace levels, in blanks. Blank corrections were not used. The spike recovery was acceptable (between 70 to 100%), and the shift (abundance of target compounds in standard solutions before and after running a batch of samples) was below the 25% limit. QA data, including blanks, lab replicates and surrogate spike recoveries, are presented in Supplemental Tables S1–S4.

The total organic carbon (OC) content was determined using the loss-on-ignition method (Wang et al., 2011a). Briefly, 2 to 4 grams of sediment was placed in a borosilicate glass beaker, heated at 105 °C for 12 h to remove moisture, and then the sample dry weight was determined. The dried sediment was then placed in a muffle furnace (Neycraft Vulcan A-550), combusted at 500 °C for 12 h, and weighed. The weight loss was multiplied by 0.58 to calculate the OC mass (Wang et al., 2011a), and the OC content was calculated as the OC mass divided by the dry sample weight times 100%. Replicates performed for seven samples gave an average RPD of 7.1%. For calibration and standard recovery tests, similar weights of L-glutamic acid (Sigma-Aldrich, St. Louis, MO) and mixture of glutamic acid and CaCO₃ (Sigma-Aldrich, St. Louis, MO) were prepared along with the samples. QA data for OC measurements, including replicates, blanks and recoveries, are in Supplemental Table S5.

2.4 Data analysis

PAH, NPAH, hopane and sterane concentrations were calculated as ng/g wet weight (ww), and then divided by (1 – moisture content) to obtain ng/g dry weight (dw). (Measurements were not corrected for spike recoveries since QA bounds were acceptable.) Sums and abundances exclude the few compounds (acenaphthene, nitrobiphenyls, 5-nitroacenaphthene, 9-nitroanthracene and 9-nitrophenanthrene) that were undetected in all samples (Table 1). Fluorene was detected above MDL in 9 of 24 samples with a maximum concentration of 1.1 ng/g dw, which was very low compared to other PAHs. Due to the low concentrations, low detection frequency and low toxicity (Nisbet and LaGoy, 1992), this compound was also excluded from the statistics (as further discussed in Section 3.1.1). For the remaining compounds (all with 100% detection frequencies), concentrations within a compound class were summed, e.g., the 14 detected PAHs, 5 detected NPAHs, 6 detected steranes and 5 detected hopanes were designated as ΣPAH_{14} , ΣNPAH_5 , $\Sigma\text{Sterane}_6$ and ΣHopane_5 , respectively. The abundance of each PAH compound was calculated as the concentration of that compound divided by the ΣPAH_{14} concentration. Abundances of NPAHs, steranes and hopanes were calculated similarly.

Concentrations of individual PAHs (ng/g dw) at each site were divided by the corresponding %OC to yield a value normalized to 1% OC. To assess potential effects on benthic organisms, the normalized concentrations were compared to consensus-based sediment quality guidelines (SQGs) (WDNR, 2003).

Concentrations of ΣPAH_{14} , ΣNPAH_5 , $\Sigma\text{Sterane}_6$ and ΣHopane_5 (ng/g dw) were plotted against OC content (Supplemental Figure S1A) and regression analyses were performed. The regression analyses excluded sites B-6 and V-1 because the sample containers broke

before OC measurements could be completed, and determinations using the available samples were not considered accurate due to lack of homogenization or contamination.

Concentrations (dry weight) were divided by their OC content to obtain OC-adjusted concentrations (expressed as $\mu\text{g/g OC}$). (Data from sites B-6 and V-1 were excluded as noted above.)

OC-adjusted concentrations across southern Lake Michigan were estimated using 2-D ordinary Kriging and a power variogram $\gamma(h_{ij}) = ah_{ij}^{1.5}$ where h_{ij} = distance between two points (Deglo De Besses, 2013), and then plotted as concentration maps using surface charts (Microsoft Excel 2013, Microsoft, Redmond, CA).

The loading rate of ΣPAH_{14} into southern Lake Michigan, L (MT/yr) was estimated as

$$L = \left[F \cdot (A \cdot 10^{10} \text{ cm}^2/\text{km}^2) \cdot \frac{100-M}{100} \cdot \frac{OC}{100} \cdot C \right] \cdot 10^{-12} \text{ t}/\mu\text{g} \quad (1)$$

where F = sedimentation rate ($\text{g}/\text{cm}^2\text{-yr}$), A = surface area of the southern portion (km^2), M = sediment moisture content (%), OC = sediment OC content (%), C = average OC-adjusted ΣPAH_{14} concentration ($\mu\text{g}/\text{g OC}$) across the study area derived from the Kriging map, and constants provide unit conversions. Loadings of ΣNPAH_5 , $\Sigma\text{Sterane}_6$ and ΣHopane_5 were calculated similarly. Further details on these parameters are provided in Section 3.1.4. Significant uncertainties can result from using a one-compartment model that assumes the average sedimentation rate, moisture content and OC content apply to all of southern Lake Michigan, as well as the Kriging-based estimates and limited data set that incompletely accounts for localized and near-shore discharges. Still, the approach using eq. (1) provides insight regarding total loadings to open water lake sediments from all sources.

Nine diagnostic source ratios between individual compounds were calculated to help identify major sources of target SVOCs, and are listed and interpreted in Table 2. Maps for each ratio were also produced using 2-D Kriging and techniques described above.

2.5 Chemical Mass Balance (CMB) modeling

CMB modeling was used to apportion PAHs in southern Lake Michigan sediments, following applications performed previously (Christensen et al., 1999; Li et al., 2003; Van Metre and Mahler, 2010). This approach assumes that the concentration of each chemical species measured at a receptor is linear combination of the contributions from various sources. The EPA-CMB v8.2 software (EPA, 2004a) with inputs including source profiles (described below) and experimentally measured PAH concentrations in Lake Michigan sediments, in $\text{ng}/\text{g dw}$ (Supplemental Table S9). The precision of each measurement, used in the model, was determined from duplicate laboratory analyses, and calculated as the average percent difference between duplicates (which ranged from 17% to 49% among the 16 PAHs) multiplied by the measured concentration.

Twelve PAH source profiles were considered (Supplemental Table S10). They include eight coal- and traffic- related profiles based on a comprehensive compilation (Li et al., 2003), an

industrial boiler profile that represents the average of four boiler types (heavy oil, diesel, heavy oil + natural gas and coke oven gas + blast furnace gas) (Li et al., 1999), and a fireplace combustion profile for burning pine wood (Schauer et al., 2001). Two profiles for coal-tar sealed pavement dust were also included: the mean profile across six cities (Minneapolis, MN; Chicago, IL; Detroit, MI; Washington, D.C.; New Haven, CT and Austin, TX), and the Chicago profile (Van Metre et al., 2008). All of these profiles used PAH measurements in the particulate phase except the boiler profile, which included both vapor and particulate phases. The profiles combined BBF and BKF given the difficulties separating these two compounds (Li et al., 2003). An uncertainty of 40% was applied to each component of each profile (Li et al., 2003; Van Metre and Mahler, 2010).

For the EPA-CMB v8.2 software, the maximum number of iterations was set at 20 (maximum allowable), and a maximum source uncertainty of 50% was used, exceeding the default (20%) given the higher uncertainties expected for PAHs in sediments due to complex transport and transformation processes (Li et al., 2003). The minimum source projection was 0.95 (default value), below which the source is considered as “inestimable,” and the option “source elimination” was selected, which eliminated physically impossible negative source contributions.

3. Results and Discussion

The physical characteristics and SVOC concentrations at the 24 Lake Michigan sediment samples are presented in Table 3, and relative abundances of individual PAHs, NPAHs and biomarkers are shown in Figure 2. Maps of OC-adjusted ΣPAH_{14} , ΣNPAH_5 , $\Sigma\text{Sterane}_6$ and ΣHopane_5 concentrations are displayed in Figure 3.

3.1 Concentrations and distributions

3.1.1 PAHs—Of the 16 target PAHs, 14 were detected at concentrations above MDLs in all samples. Acenaphthene was not detected in any sample, and fluorene was detected in only 9 of 24 samples above MDL (0.033 ng/g dw) with a maximum concentration of 1.1 ng/g dw (site B-5). Sites with detectable fluorene levels were dispersed and did not show any clear patterns. Due to its low concentrations, low detection frequency and low toxicity (toxic equivalent factor of 0.001) (Nisbet and LaGoy, 1992), fluorene was omitted from subsequent statistics. Three- and four-ring compounds were most abundant, e.g., phenanthrene, fluoranthene, pyrene and chrysene, and accounted for about 80% of ΣPAH_{14} , while five- and six-ring PAHs constituted the remainder. PAH profiles were similar across sites, as shown by Figure 2 and the correlation between concentrations at different sites (Supplemental Table S6).

ΣPAH_{14} concentrations varied from 210 to 1290 ng/g dw among sites, and were significantly correlated with OC content ($p < 0.0001$, $R = 0.79$, $n = 22$; Supplemental Figure S1A), as shown previously (Liang et al., 2007; Zhang et al., 1993). This correlation reflects the tendency for PAHs and other hydrophobic organic chemicals to sorb to organic matter in bottom sediments (Karickhoff, 1981). The OC-adjusted concentrations better reflect spatial differences in the sediments. Samples collected closest to the AOCs, specifically sites H-8, S-2, X-1, H-28 and A-1 corresponding to Waukegan Harbor, Grand Calumet, Muskegon

Lake, Kalamazoo River and the St. Joseph River estuary, respectively, had significantly higher ΣPAH_{14} concentrations ($86 \pm 43 \mu\text{g/g OC}$) than off-shore sites ($29 \pm 16 \mu\text{g/g OC}$; $t = 2.95$, $df = 4.3$, $p = 0.039$).

The concentration map (Figure 3A) shows a clear pattern of declining concentration with increasing distance from the shore. This map shows the mean values from the kriging interpolation and does not include the confidence intervals. In addition, concentrations in areas with few or no data points and near the coast can have large uncertainties. For example, the southwest near-shore regions near Chicago and Gary had the highest interpolated mean ΣPAH_{14} levels (160 to 180 $\mu\text{g/g OC}$). Gary is near an AOC, the Grand Calumet River, that is heavily contaminated with PAHs, as well as Indiana Harbor and the Ship Canal (EPA, 2013; MacDonald et al., 2002; Nevers et al., 2013). Chicago is a large and highly industrialized city with potentially significant emissions from traffic, diesel engines, coke ovens, coal combustion, wood burning (Bzdusek et al., 2004; Simcik et al., 1999), and coal-tar pavement sealcoat (Van Metre and Mahler, 2010). Measurements in sediments of the Grand Calumet region include ΣPAH_{17} levels from 123 to 500 $\mu\text{g/g OC}$ (4.9 to 20 $\mu\text{g/g dw}$, assumed 4% OC) in adjacent Lake Calumet (discharging into the Calumet River and then into Lake Michigan) (Li et al., 2003), mean ΣPAH_{16} concentrations of 1400 $\mu\text{g/g OC}$ at Indiana Ridge Marsh, 2700 $\mu\text{g/g OC}$ at the Indiana Ship Canal, 630 $\mu\text{g/g OC}$ at the Little Calumet River, and 40 $\mu\text{g/g OC}$ at Big Marsh (all converted from $\mu\text{g/g dw}$ assuming 4% OC) (Levengood and Schaeffer, 2011). These levels exceed the off-shore kriging estimates near Chicago and Gary by two- to tenfold. Since the present study uses only 24 open-water sites with water depths greater than 10 m, and no samples were taken directly areas near from AOCs and urban and industrial discharges, the mapping results apply to only open water areas. While estimated concentrations appear reasonable, additional measurements are desirable for confirmation.

Time trends are examined using data from five earlier studies that measured PAH levels in Lake Michigan surficial sediments during the 1980s and 1990s. Three studies examined open water areas (Eadie et al., 1982; Helfrich and Armstrong, 1986; Simcik et al., 1996), and two examined Green Bay (Su et al., 1998; Zhang et al., 1993), which is separated from the open water and near the industrial city of Green Bay and two AOCs. The six PAHs measured in common across the studies (phenanthrene, fluoranthene, pyrene, chrysene, benzo[a]pyrene (B[a]P), and benzo[ghi]perylene) were summed (designated ΣPAH_6) and are depicted in Figure 4. ΣPAH_6 concentrations in open water sediments declined from 1980 to 2011, and a linear regression using mean concentrations and five time points indicates an average decrease of $42 \pm 5 \text{ ng/g}$ per year (Figure 4; $R^2 = 0.96$). This trend likely reflects the decreasing PAH loadings into the lake, a result of lower airborne concentrations and atmosphere deposition rates, as observed in gaseous, particulate and precipitation sampling in Chicago (Sun et al., 2006a; Sun et al., 2006b), in vapor phase sampling at remote sites including Eagle Harbor and Sleeping Bear Dunes (Sun et al., 2006b), and as derived from sediment cores (Schneider et al., 2001; Simcik et al., 1996). The decline has been attributed to the transition from coal to oil and natural gas, controls on industrial emissions, reduced coke production, and changed coking technology (Schneider et al., 2001; Simcik et al., 1996); it may also reflect decreased emission rates from vehicles occurring since the 1970s (Beyea et al., 2008). The trend also might reflect analytical changes that have increased the

resolution and sensitivity of measurements; sampling and analysis of sediment cores would be useful to confirm results.

Green Bay sediments have higher ΣPAH_6 concentrations that do not fit the trend line in Figure 4. Green Bay is near two AOCs (Menominee River and Fox River Lower Green Bay) and an industrial city. High PAH concentrations due to coal tar wastes have been detected in Menominee River sediments, and leaking underground storage tanks have been a concern for the lower Fox River Basin (EPA, 2013). The proximity to PAH sources likely explains the higher PAH concentrations seen these sediments.

The PAH concentrations in open water sediments of southern Lake Michigan in the present study (210 to 1290 ng/g dw) are generally comparable to levels elsewhere, although lower than levels in highly polluted areas. For example, sediment ΣPAH_{19} concentrations in Isle Royale National Park, Lake Superior ranged from 17 to 346 ng/g dw at background sites, and 1516 to 3410 ng/g at marinas and docks (Cox and Clements, 2013). Sediment ΣPAH_{13} concentrations reached 14 $\mu\text{g/g}$ dw in Detroit River, but ranged from 0.25 to 2.0 $\mu\text{g/g}$ in other parts of the Huron-Erie Corridor (Szalinska et al., 2011). In two headwater lakes of the Athabasca Oil Sands Region, Canada, ΣPAH_{16} concentrations ranged from 100 to 320 ng/g dw throughout the sediment cores (Jautzy et al., 2013). ΣPAH_{15} concentrations in Lake Taihu sediments in highly populated eastern China were 209 to 1003 ng/g dw (Zhang et al., 2012). Surface sediments from Lake Koumoundourou, Greece had ΣPAH_{14} concentrations from 780 to 3600 ng/g dw (Hahladakis et al., 2013).

Normalized PAH concentrations were compared to consensus-based SQGs to assess potential effects on benthic organisms using recommendations by the Wisconsin Department of Natural Resources (WDNR, 2003) (Supplemental Table S8). For most individual PAHs and the PAH sum, concentrations were lower than threshold effect concentrations (TECs), indicating that the toxicity effect to benthic-dwelling organisms is unlikely. However, concentrations of pyrene, chrysene, and dibenzo[a,h]anthracene at site S-2 (259, 187, and 36 ng/g, respectively), and pyrene, benz[a]anthracene and chrysene at site H-28 (193, 134, and 183 ng/g) exceeded TECs, as did dibenzo[a,h]anthracene at sites A-1 and H-15 (47 and 38 ng/g). However, concentrations were much lower than midpoint effect concentrations (MECs) and probable effect concentrations (PECs), suggesting a low risk to the benthic organisms. The B[a]P toxic equivalents were not calculated for these samples given that the bottom sediments were too deep for human exposure and no other human exposure pathway was plausible.

3.1.2 NPAHs—Five of the 11 target NPAHs (1-nitronaphthlene, 2-nitronaphthalene, 2-nitrofluorene, 1-nitropyrene and 6-nitrochrysene) were detected above MDLs in all samples; the six other NPAHs were never detected. ΣNPAH_5 concentrations ranged from 2.9 to 18.6 ng/g dw (Table 3), roughly 10 to 100 times lower than the ΣPAH_{14} concentrations. (NPAH data at each site are presented in Supplemental Table S13). The two most abundant compounds, 1-nitropyrene and 6-nitrochrysene, respectively comprised an average of 33% and 40% of the ΣNPAH_5 concentration (Figure 2B). The abundance of 6-nitrochrysene is noteworthy given its high carcinogenic potency, i.e., toxic equivalent factor or TEF = 10

relative to B[a]P (RIDEM, 2008). Average abundances of the other NPAHs detected were below 10%.

Like the PAHs, Σ NPAH₅ levels were significantly correlated with OC content ($p < 0.0001$, $R^2 = 0.85$, $n = 22$, Supplemental Figure S1B). OC-adjusted Σ NPAH₅ concentrations were higher at sites near AOCs and urban/industrial areas ($1.33 \pm 0.95 \mu\text{g/g OC}$) compared to other sites ($0.43 \pm 0.28 \mu\text{g/g OC}$; Mann-Whitney $U = 10$, $p = 0.005$). The concentration map again shows declining concentrations with increasing distance from the shore, and high concentrations near source areas (Chicago/Gary and Kalamazoo River) (Figure 3B), suggesting that urban and industrial sources are important in near-shore environments. Again, the map shows only mean values, and near shore areas are subject to large uncertainties. 2-Nitronaphthalene, 1-nitropyrene and 6-nitrochrysene were highly correlated with each other, while 1-nitronaphthalene was significantly correlated with 2-nitrofluorene (Supplemental Table S6).

NPAH concentrations in the low ng/g range have been reported in several studies examining both freshwater and marine sediments. Σ NPAH₅ (1- and 2-nitronaphthalenes, 1-nitropyrene, 6-nitrochrysene and 9-nitrophenanthrene) in Elbe river, Germany and Czech Republic ranged from 5.4 to 14.9 ng/g (Lubcke-von Varel et al., 2011). In sediments of the Suimon River, Japan, 1-nitropyrene and 2-nitrofluorene averaged 25 and 1.5 ng/g, respectively (Sato et al., 1985). Marine coastal sediments near Barcelona, Spain had 1-nitropyrene and 6-nitrochrysene concentrations of 0.68 and 0.52 ng/g dw, respectively (Fernandez et al., 1992). Σ NPAH₃ (9-nitroanthracene, 1-nitropyrene and 6-nitrochrysene) concentrations in Hiroshima Bay, Japan averaged 2.2 ng/g dw ($n=11$; range: 0.25 to 7.34) (Ozaki et al., 2010). These levels are roughly comparable to those measured in southern Lake Michigan in the present study (Σ NPAH₅ average of 8.0 ± 3.9 ng/g, range from 2.9–18.6 ng/g dw, $n = 24$). Much higher levels were measured in sediments of a small municipal stormwater settling pond in Varney Pond, MN, e.g., 1-nitropyrene, 2-nitrofluorene and 6-nitrochrysene ranged from 19–120, 40–710, and 73–150 $\mu\text{g/g dw}$, respectively (MDH, 2011), which suggests the significance of urban runoff sources.

3.1.3 Biomarkers—All target hopanes and steranes in all samples were detected above MDLs. Σ Hopane₅ concentrations ranged from 98 to 355 ng/g dw and Σ Sterane₆ levels from 6.2 to 36 ng/g dry weight. Like PAHs and NPAHs, levels were correlated with OC content ($p < 0.0001$, $R = 0.80$ and 0.83 for steranes and hopanes, respectively; $p < 0.0001$) (Supplemental Figures S1C and D). OC-adjusted Σ Sterane₆ and Σ Hopane₅ concentrations displayed spatial patterns similar to the PAHs (Figures 3C and 3D), and concentrations were significantly higher near source areas (sites H-8, S-2, X-1, H-28 and A-1) than other sites (for Σ Hopane₅: Mann-Whitney $U = 12$, $p = 0.009$; for Σ Sterane₆: $t = 2.62$, $df = 4.41$, $p = 0.053$). Among steranes, 20R-5 α (H),14 β (H),17 β (H)-24-methylcholestane and 20R-5 α (H),14 β (H),17 β (H)-cholestane were most abundant, contributing to 36% and 23% of the total, respectively. Among hopanes, 17 α (H),21 β (H)-hopane was most abundant (35% of Σ Hopane₅); the four other hopanes had similar contributions (16–17%). The profiles of the biomarkers were similar across sites (Figure 4), and individual hopane and sterane compounds were significantly correlated to each other (Supplemental Table S7).

3.1.4 Loading rates of SVOCs—The loading rate of ΣPAH_{14} to open water sediments of southern Lake Michigan, estimated using eq. (1), the spatial average OC-adjusted ΣPAH_{14} concentration (41 $\mu\text{g/g}$ OC), a mass sedimentation rate of 0.0356 $\text{g/cm}^2\text{-yr}$ for southern Lake Michigan (Corcoran, 2013), the average moisture content of 41.5% and OC content of 2.2% (this study), and the estimated surface area of the southern portion (21600 km^2), is 4.1 t/yr. Although we did not measure concentrations in the northern portion of the lake, an approximate lake-wide loading rate is calculated by scaling up to the entire Lake surface area (58000 km^2), which gives a ΣPAH_{14} loading of 10.9 t/yr. Using the same approach, lake-wide loadings of ΣNPAH_5 , $\Sigma\text{Sterane}_6$ and ΣHopane_5 are 0.16, 0.25 and 3.6 t/yr, respectively. The historical decline in PAH levels must be considered to compare these results to earlier loading estimates. A 1980 estimate of PAH loadings to Lake Michigan, obtained by summing the PAH inputs from various sources (some of which had inconsistent PAH species) is 50 to 55 t/yr (Helfrich and Armstrong, 1986). Using the regression line for PAH levels in Lake Michigan sediments shown in Figure 4, ΣPAH_6 concentration in 1980 (1679 ng/g dw) was 4.6 times the level in 2011 (368 ng/g dw). Assuming that ΣPAH_{14} concentrations follow the ΣPAH_6 trend, and that sedimentation rate, sediment moisture content, and OC content are unchanged, then the ΣPAH_{14} loading rate in 1980 would be 4.6 times the current (2011) loading or 50.6 t/yr, within the range reported for 1980. A second and independent estimate of PAH loadings, based on accumulation profiles in sediment cores sampled in 1991–1993 (and calculated using a ΣPAH_{17} deposition rate = 50–70 $\text{ng/cm}^2\text{-yr}$ and area = 58000 km^2), is 29 to 41 t/yr (Simcik et al., 1996). For 1992, we estimate a ΣPAH_{14} loading rate of 35.2 t/yr, again within the reported range.

While the estimated ΣPAH_{14} loading rates agree well with the earlier estimates, uncertainties and possible errors in our estimates are recognized. Overall, the southern portion of the lake is more polluted than the northern, thus applying the average concentration in the southern portion to the whole lake may overestimate loadings. However, this may be offset since near-shore areas that tend to have higher concentrations were under-sampled. Second, sedimentation rate, sediment moisture content and OC content can vary across sites, and applying the average data from the southern portion to the whole lake may be inaccurate. Third, sampling and measurement variation can affect results, although open water sediment samples provide a high degree of spatial and temporal representativeness, particularly compared to airborne and deposition samples that can vary considerably. Given the difficulty in assessing these factors, especially the extrapolation to the whole lake, no quantitative estimates of uncertainty is provided. Despite these concerns, our loading estimates show remarkable agreement with earlier estimates that used independent methods. Moreover, the stability and representativeness of sediment samples suggests that this approach for estimating SVOC loadings is useful and applicable to other persistent and sediment-bound contaminants. However, the uncertainties of the approach, especially in near shore areas, should be recognized.

3.2 Source identification

3.2.1 PAHs

Diagnostic ratios: PAH sources contributing to southern Lake Michigan sediments are identified using abundances and ratios of individual compounds, which serve as source

indicators. Eight diagnostic ratios for identifying PAH sources (Table 4) are used to help identify sources. These ratios are semi-quantitative (i.e., numerical apportionments are not provided), and they are most useful when there is a single dominating source, which is unlikely in a large region like Lake Michigan. In addition, the ratios can be influenced by atmospheric reactions and selective loss processes, and thus may provide contradictory or inconsistent results (Katsoyiannis et al., 2011). Despite such limitations, the ratios can provide useful insights to contributing sources.

The BAA/CHR ratio indicates urban influences by reflecting differences in the susceptibility to photo-oxidation (Table 2) (Gschwend and Hites, 1981). The average BAA/CHR ratio (0.72 ± 0.23) is comparable with previous studies and within the range reported for sediments collected near urban areas (Gschwend and Hites, 1981; Helfrich and Armstrong, 1986). Site B4, most distant from urban sources (54 km from shore, 54 km from Benton Harbor and 175 km from Chicago), had the second lowest BAA/CHR ratio (0.57). However, this ratio was not significantly correlated with either distance from shore or to AOCs, industrial or urban areas, and there was no clear spatial pattern (see Supplemental Figures S2C), as has been noted previously (Helfrich and Armstrong, 1986). This lack of correlation can arise from several factors. First, the southern Lake Michigan contains several cities/harbors/AOCs, and the off-shore samples likely are affected by multiple sources. Second, this ratio does not apply to waterborne transport, e.g., materials discharged or deposited in near-shore areas and then transported and distributed to sediments (Simcik et al., 1999). Third, there is movement and redistribution of surface sediments in southern Lake Michigan (Corcoran, 2013). Finally, as noted, this ratio could be influenced by other physiochemical processes (Katsoyiannis et al., 2011).

The remaining seven PAH ratios indicate petrogenic or pyrogenic sources (Table 2) (Budzinski et al., 1997; Wang et al., 2006; Yunker et al., 2002). PHE/ANT and FLA/PYR ratios are usually used simultaneously (Budzinski et al., 1997). A plot of PHE/ANT vs. FLA/PYR ratios suggests that pyrogenic (i.e., combustion) sources are the main contributor of PAHs at most (N=14) sites (Figure 5). Seven sites reflect a combination of petrogenic and pyrogenic sources. Three sites are in the petrogenic zone, but at the boundary, suggesting significant contributions from pyrogenic sources. The ANT/178 ratio averaged 0.12 ± 0.04 (N = 24) and several sites had ratios just slightly below 0.10. The FLA/202 ratio averaged 0.54 ± 0.13 (n=24); 17 sites had ratios >0.50; six sites had ratios between 0.40 and 0.50; and only one site had a ratio <0.4. All sampling sites had BAA/228 ratios above 0.35, IND/276 ratios above 0.50, and Σ LPAHs/ Σ HAPAHs ratios below 1. Together, these ratios suggest the dominance of combustion sources, especially coal and/or wood combustion, with some contribution from liquid fossil fuel combustion, i.e., vehicle emissions.

Although the PAH diagnostic ratios are qualitative and have limitations, they consistently identify pyrogenic sources as the major contributors of PAHs to southern Lake Michigan sediments. This is in accordance with previous apportionment studies, which identified traffic emissions, coal combustion and wood burning as major sources (Bzdusek et al., 2004; Christensen and Arora, 2007; Simcik et al., 1996).

CMB results: Colinearity among the twelve PAH source profiles and the mean PAH profile in southern Lake Michigan sediments initially, initially evaluated using Pearson correlation coefficients (Supplemental Table S11), showed several profiles were similar to the 24-site average profile, including those for coal-tar Chicago, pine-wood combustion, power plant, traffic average, and diesel engine exhaust ($r = 0.93, 0.91, 0.89, 0.89$ and 0.87 , respectively). Several source profiles were significantly correlated, suggesting the possibility of multicollinearity issues, e.g., unstable source estimates and convergence issues. To investigate and help account for such concerns, ten CMB models using different fitting species and subsets of source profiles were tested. Each was run 24 times (one for each site), and the “preferred” model discussed here was selected as the model that converged at all 24 sites and showed good performance in terms of R^2 , χ^2 and percentage of Σ PAH mass explained (Supplemental Table S12). This model included four sources: coal-fired power plant, coke oven, diesel engine and coal-tar pavement dust Chicago. Since all four traffic-related profiles were highly correlated, the diesel engine profile is considered to represent traffic-related sources. Including industrial boiler and pine-wood combustion profiles caused convergence issues at many sites. This model included nine fitting species, specifically, PHE to BGP with the exceptions of ANT and BAP, two compounds that have are highly reactive in the atmosphere (Gschwend and Hites, 1981; Li et al., 2003).

Using the selected four-source model, diesel engine exhaust was identified at all sites as the most significant source, contributing to $56 \pm 18\%$ of the Σ PAHs; coal power plant emissions were identified (source contribution larger than zero) at 22 sites, contributing $27 \pm 14\%$; coal-tar sealed pavement dust was identified at 19 sites with a $16 \pm 11\%$ contribution; and coke oven was detected at 11 sites with a $7 \pm 12\%$ contribution (Supplemental Table S12). These results are consistent with the diagnostic ratios as well as previous apportionment studies highlighting the importance of traffic emissions and coal combustion (Bzdusek et al., 2004; Christensen and Arora, 2007; Simcik et al., 1996). While coal-tar sealed pavement dust was identified, its contribution was low compared to the 57% estimated for urban lakes in the eastern U.S. (Van Metre and Mahler, 2010), possibly reflecting the significance of atmospheric deposition in Lake Michigan as compared to urban runoff, the principal pathway for coal-tar sealcoat dust.

Across the 24 sites, the CMB model performance was reasonable, e.g., R^2 , χ^2 and percentage mass explained averaged 0.81, 3.1 and 106%, respectively (Supplemental Table S12). However, CMB apportionments in urban lakes have attained better performance, e.g., $R^2 > 0.9$ and $\chi^2 < 2$ (Li et al., 2003; Van Metre and Mahler, 2010). Given the potentially longer transport distances and times relevant to Lake Michigan, the assumption that profiles remain constant from source to receptor (sampled sediment) (EPA, 2004b) may not reflect chemical, photochemical and biological degradation, as well as partitioning, that occurs during atmospheric transport, deposition and sediment burial (Galarneau, 2008; Li et al., 2003). These concerns may be mitigated for urban lakes near sources. Target transformation and other techniques (Pistikopoulos et al., 1990; Thurston and Spengler, 1985) might be used to help address such issues.

3.2.2 NPAHs—Few diagnostic source ratios are available for NPAHs. The 1-NPYR/PYR ratio has been used to distinguish contributions of diesel-engine vehicles and coal

combustion emissions in both atmospheric particulate matter and marine sediments (Ozaki et al., 2010; Tang et al., 2005). This ratio is approximately 0.001 for lower temperature (900 °C) coal stove emissions, and 0.36 for higher temperature (2700 °C) diesel engine exhaust (Tang et al., 2005). Although the type of coal stove sampled was not stated, this ratio may apply to coal combustion in smaller furnaces that have lower temperatures than diesel engines. Coal and wood stoves/fireplaces are used for residential heating or aesthetics around Lake Michigan area, although wood stoves may be more popular. In Lake Michigan sediments, the 1-NPYR/PYR ratio averaged 0.03 ± 0.01 (range from 0.01 to 0.08, N = 24, Table 4), which is comparable to levels reported in marine sediments (0.017 – 0.023) (Ozaki et al., 2010), suggesting a combination of diesel engine and coal combustion emissions, consistent with the sources identified for the parent PAHs. This ratio showed a complex spatial pattern (Supplemental Figure S2H), possibly due to the instability of diagnostic ratios in the environment, as discussed above.

The NPAH profiles provide additional source information. In Lake Michigan sediments, 1-nitropyrene and 6-nitrochrysene were the predominant compounds, followed by 2-nitrofluorene. In the atmosphere, these compounds are primarily emitted by diesel vehicles (Albinet et al., 2007; Bamford and Baker, 2003; Reisen and Arey, 2005), and an airborne 2-nitrofluorene concentration equal to 15% of that of 1-nitropyrene is commonly observed (Albinet et al., 2007). Thus, levels of these compounds suggest contribution from diesel engine exhaust. On the other hand, sediment concentrations of 6-nitrochrysene were slightly higher than those of 1-nitropyrene, while concentrations of 6-nitrochrysene generally are lower than those of 1-nitropyrene in diesel and gasoline engine emissions, tire debris and asphalt paste (Khalek et al., 2011; Ozaki et al., 2010). However, atmospheric formation of 6-nitrochrysene has been shown by exposing chrysene to 10 ppm of nitrogen dioxide (NO₂) (Tokiwa et al., 1981). Chrysene is a marker of coal combustion (Harrison et al., 1996), and the most abundant PAH in coal power plant emissions (Bzdusek et al., 2004). States surrounding Lake Michigan, including Illinois and Indiana, have numerous coal-fired power plants. Thus, we speculate that a portion of the chrysene emitted from coal combustion sources undergoes atmospheric transformation into 6-nitrochrysene, followed by deposited in the lake and incorporation into sediments. However, further studies are needed to confirm this pathway.

3.2.3 Biomarkers—Anthropogenic sources of hopanes and steranes in Lake Michigan include crude oil and derived products, e.g., engine lubricating oil. Although major oil spills have not been reported in southern Lake Michigan, it may be subject to some oil spillage since Indiana Harbor and Chicago are major distribution centers for petroleum products (Helfrich and Armstrong, 1986). In addition, hopanes and steranes are present in lubricating oils of diesel and gasoline engines, and are components of vehicle exhaust (Khalek et al., 2011; Liu et al., 2010; Schauer et al., 1999; Schauer et al., 2002). Similarly, outboard motor oil and exhaust from ships/boats are potential sources (Bieger et al., 1996). Sediments can also reflect natural sources of hopanes and steranes including decomposition of bacteria, algae and vascular plants (Qu et al., 2007; Xiong et al., 2010).

Unlike PAHs and NPAHs, diagnostic ratios of hopanes and steranes cannot distinguish between petrogenic and pyrogenic sources because these compounds are largely conserved

during combustion and environmental transport (Manan et al., 2011; Neff and Durell, 2012). However, these ratios can distinguish petrogenic and biogenic hydrocarbons (Hostettler et al., 1992; Neff and Durell, 2012; Qu et al., 2007; van Dongen et al., 2008). One such ratio can be calculated considering the hopanes and steranes measured in the present study. This ratio, $C_{31-22S}/(22S+22R)$, compares two diastereomers of C_{31} -homohopanes ($17\alpha(h)$, $21\beta(h)$ -homohopanes), and a value of 0.6 indicates equilibrium or full maturity, i.e., petroleum (Table 2). In Lake Michigan, this ratio ranged from 0.37 to 0.65; four sites had ratios >0.6 ; seven sites had ratios from 0.5 – 0.6; and 13 sites had ratios <0.5 . The ratio map shows that the lower half of the study area tends to have ratios >0.5 , while the upper half generally displays ratios <0.5 (Supplemental Figure S2I). This suggests that the southern end of the lake was significantly impacted by petroleum (crude oil, vehicle emissions, etc.), while biogenic inputs (vascular plants, microbes) become more important in the central and northern parts. While consistent with earlier results, the ratio map does not represent sampling and analytical variability, and a single diagnostic ratio might not be robust, thus, measurement of additional compounds and calculation of several diagnostic ratios in future studies would help to confirm results.

4. Conclusions

Four groups of SVOCs were measured in sediments collected at 24 off-shore sites in southern Lake Michigan of varying water depths and sediment types. Compared to the 3–5 sampling sites used in previous studies, data from 24 sites better describe the spatial patterns and the influence of potential source areas, and provide more robust estimates of levels across the lake. ΣPAH_{14} concentrations, which ranged from 210 to 1290 ng/g dw, were highest at near-shore industrialized and contaminated areas. Overall, PAH levels in sediments have been declining for the past three decades, and only low risks to benthic organisms are indicated using consensus-based SQGs. We provide the first report of NPAHs in Lake Michigan sediments. $\Sigma NPAH_5$ concentrations ranged from 3 to 19 ng/g dw, and several highly toxic compounds were detected, including 6-nitrochrysene. $\Sigma Hopane_5$ and $\Sigma Sterane_6$ concentrations ranged from 98 to 355 ng/g and 6 to 36 ng/g dw, respectively, and several petroleum-specific hopanes were detected. OC-adjusted SVOC concentrations increase at locations near AOCs and larger urban/industrial areas.

The estimated 2011 loading rates of ΣPAH_{14} , $\Sigma NPAH_5$, $\Sigma Sterane_6$ and $\Sigma Hopane_5$ to open water sediments of Lake Michigan are 10.9, 0.16, 0.25 and 3.6 t/yr, respectively. The PAH loading estimate has excellent agreement with prior estimates obtained using different and independent methods; loading rates for the other three compound groups are the first presented in the literature. Relative abundances were similar across sites, indicating that common source types affected sediments across southern Lake Michigan. Based on diagnostic ratios and chemical mass balance modeling, PAHs were contributed by primarily pyrogenic sources, e.g., coal combustion and vehicle exhaust; coal-tar sealed pavement dust was also identified. Based on hopane biomarkers, both petroleum-derived and biogenic sources are important contributors of hydrocarbons in sediments. Finally, NPAH compounds with high carcinogenic potencies (e.g., 6-nitrochrysene) were measured at modest concentrations in sediments, suggesting that an assessment of ecological risks may be warranted.

Supplementary Material

Refer to Web version on PubMed Central for supplementary material.

Acknowledgments

The authors thank Thomas Nalepa and other personnel at the National Oceanic and Atmospheric Administration Great Lakes Environmental Research Laboratory for collection of sediment samples. We also thank Dongyan Sun for helping with the processing and analysis of sediment samples. This study was supported in part by US EPA grant GL00E00690-0, entitled PAHs, Nitro-PAHs & Diesel Exhaust Toxics in the Great Lakes: Apportionments, Impacts and Risks. The National Institute of Environmental Health Sciences, National Institutes of Health provided additional support in grant P30ES017885 entitled Lifestage Exposures and Adult Disease.

References

1. Albinet A, Leoz-Garziandia E, Budzinski H, Villenave E. Polycyclic aromatic hydrocarbons (PAHs), nitrated PAHs and oxygenated PAHs in ambient air of the Marseilles area (South of France): concentrations and sources. *Science of the Total Environment*. 2007; 384:280–292. [PubMed: 17590415]
2. Andren, AW.; Strand, J. Atmospheric deposition of particulate organic carbon and polyaromatic hydrocarbon to Lake Michigan. In: Eisenreich, SJ., editor. *Atmospheric Pollutants in Natural Waters*. Ann Arbor Sciecn; Ann Arbor, MI: 1979. p. 459-479.
3. ATSDR. Toxicological Profile for Polycyclic Aromatic Hydrocarbons (PAHs) (Update). Atlanta, GA: Agency for Toxic Substances and Disease Registry; 1995.
4. Baek S, Field R, Goldstone M, Kirk P, Lester J, Perry R. A review of atmospheric polycyclic aromatic hydrocarbons: sources, fate and behavior. *Water, air, and soil pollution*. 1991; 60:279–300.
5. Bamford HA, Baker JE. Nitro-polycyclic aromatic hydrocarbon concentrations and sources in urban and suburban atmospheres of the Mid-Atlantic region. *Atmospheric Environment*. 2003; 37:2077–2091.
6. Beyea J, Stellman SD, Hatch M, Gammon MD. Airborne Emissions from 1961 to 2004 of Benzo [a] pyrene from US Vehicles per km of Travel Based on Tunnel Studies. *Environmental science & technology*. 2008; 42:7315–7320. [PubMed: 18939564]
7. Bieger T, Hellou J, Abrajano TA. Petroleum biomarkers as tracers of lubricating oil contamination. *Marine Pollution Bulletin*. 1996; 32:270–274.
8. Boitsov S, Petrova V, Jensen HK, Kursheva A, Litvinenko I, Chen Y, et al. Petroleum-related hydrocarbons in deep and subsurface sediments from South-Western Barents Sea. *Marine environmental research*. 2011; 71:357–368. [PubMed: 21601919]
9. Budzinski H, Jones I, Bellocq J, Pierard C, Garrigues P. Evaluation of sediment contamination by polycyclic aromatic hydrocarbons in the Gironde estuary. *Marine chemistry*. 1997; 58:85–97.
10. Bzdusek PA, Christensen ER, Li A, Zou Q. Source apportionment of sediment PAHs in Lake Calumet, Chicago: Application of factor analysis with nonnegative constraints. *Environmental science & technology*. 2004; 38:97–103. [PubMed: 14740723]
11. CFR. Code of Federal Regulations Title 40 Part 423 Appendix A: 126 Priority Pollutants. U.S. National Archives and Records Administration; Washington, D.C: 1982.
12. Christensen ER, Arora S. Source apportionment of PAHs in sediments using factor analysis by time records: Application to Lake Michigan, USA. *Water Research*. 2007; 41:168–176. [PubMed: 17081587]
13. Christensen ER, Rachdawong P, Karls JF, Camp RPV. PAHs in sediments: Unmixing and CMB modeling of sources. *Journal of Environmental Engineering*. 1999; 125:1022–1032.
14. Corcoran, MB. Earth and Environmental Sciences. Master of Science. University of Illinois; Chicago: 2013. Variations in Sedimentation Rate and Sediment Focusing in Lake Michigan Using Radionuclide Profiles.

15. Cox ON, Clements WH. An integrated assessment of polycyclic aromatic hydrocarbons (PAHs) and benthic macroinvertebrate communities in Isle Royale National Park. *Journal of Great Lakes Research*. 2013; 39:74–82.
16. Crane JL. Source Apportionment and Distribution of Polycyclic Aromatic Hydrocarbons, Risk Considerations, and Management Implications for Urban Stormwater Pond Sediments in Minnesota, USA. *Archives of environmental contamination and toxicology*. 2014;176–200. [PubMed: 24310205]
17. Crane, JL.; Grosenheider, K.; Wilson, CB. Contamination of stormwater pond sediments by polycyclic aromatic hydrocarbons (PAHs) in Minnesota: The role of coal tar-based sealcoat products as a source of PAHs. Minnesota Pollution Control Agency; 2010.
18. de Castro Vasconcellos P, Sanchez-Ccoyllo O, Balducci C, Mabilia R, Cecinato A. Occurrence and concentration levels of nitro-PAH in the air of three Brazilian cities experiencing different emission impacts. *Water, Air, and Soil Pollution*. 2008; 190:87–94.
19. De Vault DS, Hesselberg R, Rodgers PW, Feist TJ. Contaminant trends in lake trout and walleye from the Laurentian Great Lakes. *Journal of Great Lakes Research*. 1996; 22:884–895.
20. Deglo De Besses, B. XonGrid 3 Interpolation Add-in. 2013. <http://xongrid.sourceforge.net>
21. Eadie BJ, Landrum PF, Faust W. Polycyclic aromatic hydrocarbons in sediments, pore water and the amphipod *Pontoporeia hoyi* from Lake Michigan. *Chemosphere*. 1982; 11:847–858.
22. EPA. Assessment and Remediation of Contaminated Sediments (ARCS) Program: Final Summary Report. U.S. Environmental Protection Agency; 1994.
23. EPA. Lake Michigan Lakewide Management Plan. U.S. Environmental Protection Agency; 2000.
24. EPA. Chemical Mass Balance Model EPA-CMB8.2. U.S. Environmental Protection Agency; Washington, D.C: 2004a. http://www.epa.gov/scram001/receptor_cmb.htm
25. EPA. EPA-CMB8.2 Users Manual. U.S. Environmental Protection Agency, Office of Air Quality Planning and Standards; Research Triangle Park, NC: 2004b. EPA-452/R-04-011
26. EPA. National Coastal Condition Assessment: Laboratory Methods Manual. United States Environmental Protection Agency, Office of Water; Washington, D.C: 2010.
27. EPA. Great Lakes Areas of Concern. U.S. Environmental Protection Agency; Washington, D.C: 2013. <http://www.epa.gov/glnpo/aoc/>
28. EPA&EC. Great Lakes Binational Toxics Strategy: Canada - United States Strategy for the Virtual Elimination of Persistent Toxic Substances in the Great Lakes. U.S. Environmental Protection Agency & Environmental Canada; 2004.
29. Fernandez P, Grifoll M, Solanas AM, Bayona JM, Albaiges J. Bioassay-directed chemical analysis of genotoxic components in coastal sediments. *Environmental science & technology*. 1992; 26:817–829.
30. Galarneau E. Source specificity and atmospheric processing of airborne PAHs: implications for source apportionment. *Atmospheric Environment*. 2008; 42:8139–8149.
31. Ghosh U, Zimmerman JR, Luthy RG. PCB and PAH speciation among particle types in contaminated harbor sediments and effects on PAH bioavailability. *Environmental science & technology*. 2003; 37:2209–2217. [PubMed: 12785527]
32. Gschwend PM, Hites RA. Fluxes of polycyclic aromatic hydrocarbons to marine and lacustrine sediments in the northeastern United States. *Geochimica et Cosmochimica Acta*. 1981; 45:2359–2367.
33. Hahladakis J, Smaragdaki E, Vasilaki G, Gidaracos E. Use of Sediment Quality Guidelines and pollution indicators for the assessment of heavy metal and PAH contamination in Greek surficial sea and lake sediments. *Environmental monitoring and assessment*. 2013; 185:2843–2853. [PubMed: 22821321]
34. Harrison RM, Smith D, Luhana L. Source apportionment of atmospheric polycyclic aromatic hydrocarbons collected from an urban location in Birmingham, UK. *Environmental Science & Technology*. 1996; 30:825–832.
35. Hayakawa K, Tang N, Akutsu K, Murahashi T, Kakimoto H, Kizu R, et al. Comparison of polycyclic aromatic hydrocarbons and nitropolycyclic aromatic hydrocarbons in airborne particulates collected in downtown and suburban Kanazawa, Japan. *Atmospheric Environment*. 2002; 36:5535–5541.

36. Helfrich J, Armstrong DE. Polycyclic aromatic hydrocarbons in sediments of the southern basin of Lake Michigan. *Journal of Great Lakes Research*. 1986; 12:192–199.
37. Hostettler FD, Rapp JB, Kvenvolden KA. Use of geochemical biomarkers in bottom sediment to track oil from a spill, San Francisco Bay, California. *Marine pollution bulletin*. 1992; 24:15–20.
38. Huang L, Bohac SV, Chernyak SM, Batterman SA. Composition and Integrity of PAHs, Nitro-PAHs, Hopanes, and Steranes in Diesel Exhaust Particulate Matter. *Water, Air, & Soil Pollution*. 2013; 224:1–14.
39. Jautzy J, Ahad JM, Gobeil C, Savard MM. Century-long source apportionment of PAHs in Athabasca oil sands region lakes using diagnostic ratios and compound-specific carbon isotope signatures. *Environmental science & technology*. 2013; 47:6155–6163. [PubMed: 23668471]
40. Kannan K, Lee Kober J, Kang YS, Masunaga S, Nakanishi J, Ostaszewski A, et al. Polychlorinated naphthalenes, biphenyls, dibenzo-p-dioxins, and dibenzofurans as well as polycyclic aromatic hydrocarbons and alkylphenols in sediment from the Detroit and Rouge Rivers, Michigan, USA. *Environmental Toxicology and Chemistry*. 2001; 20:1878–1889. [PubMed: 11521813]
41. Karickhoff SW. Semi-empirical estimation of sorption of hydrophobic pollutants on natural sediments and soils. *Chemosphere*. 1981; 10:833–846.
42. Katsoyiannis A, Sweetman AJ, Jones KC. PAH molecular diagnostic ratios applied to atmospheric sources: a critical evaluation using two decades of source inventory and air concentration data from the UK. *Environmental science & technology*. 2011; 45:8897–8906. [PubMed: 21859122]
43. Kemble N, Hardesty D, Ingersoll C, Johnson B, Dwyer F, MacDonald D. An evaluation of the toxicity of contaminated sediments from Waukegan Harbor, Illinois, following remediation. *Archives of environmental contamination and toxicology*. 2000; 39:452–461. [PubMed: 11031305]
44. Khalek IA, Bougher TL, Merritt PM, Zielinska B. Regulated and unregulated emissions from highway heavy-duty diesel engines complying with US Environmental Protection Agency 2007 emissions standards. *Journal of the Air & Waste Management Association*. 2011; 61:427–442. [PubMed: 21516938]
45. Kleeman MJ, Riddle SG, Robert MA, Jakober CA. Lubricating oil and fuel contributions to particulate matter emissions from light-duty gasoline and heavy-duty diesel vehicles. *Environmental Science & Technology*. 2007; 42:235–242. [PubMed: 18350902]
46. Kruege M, Mukhopadhyay P, Lewis C. A molecular evaluation of contaminants and natural organic matter in bottom sediments from western Lake Ontario. *Organic geochemistry*. 1998; 29:1797–1812.
47. Kveseth K, Sortland B, Bokn T. Polycyclic aromatic hydrocarbons in sewage, mussels and tap water. *Chemosphere*. 1982; 11:623–639.
48. Levengood JM, Schaeffer DJ. Polycyclic aromatic hydrocarbons in fish and crayfish from the Calumet region of southwestern Lake Michigan. *Ecotoxicology*. 2011; 20:1411–1421. [PubMed: 21594573]
49. Li A, Jang JK, Scheff PA. Application of EPA CMB8, 2 model for source apportionment of sediment PAHs in Lake Calumet, Chicago. *Environmental Science & Technology*. 2003; 37:2958–2965. [PubMed: 12875401]
50. Li CT, Mi HH, Lee WJ, You WC, Wang YF. PAH emission from the industrial boilers. *Journal of hazardous materials*. 1999; 69:1–11. [PubMed: 10502602]
51. Liang Y, Tse M, Young L, Wong M. Distribution patterns of polycyclic aromatic hydrocarbons (PAHs) in the sediments and fish at Mai Po Marshes Nature Reserve, Hong Kong. *Water Research*. 2007; 41:1303–1311. [PubMed: 17258265]
52. Librando V, Fazzino S. Quantification of polycyclic aromatic hydrocarbons and their nitro derivatives in atmospheric particulate matter of Augusta city. *Chemosphere*. 1993; 27:1649–1656.
53. Liu ZG, Berg DR, Vasys VN, Dettmann ME, Zielinska B, Schauer JJ. Analysis of C1, C2, and C10 through C33 particle-phase and semi-volatile organic compound emissions from heavy-duty diesel engines. *Atmos Environ*. 2010; 44:1108–1115.
54. Lübcke-von Varel U, Bataineh M, Lohrmann S, Löffler I, Schulze T, Flückiger-Isler S, et al. Identification and quantitative confirmation of dinitropyrenes and 3-nitrobenzanthrone as major

- mutagens in contaminated sediments. *Environment international*. 2012; 44:31–39. [PubMed: 22336528]
55. Lubcke-von Varel U, Machala M, Ciganek M, Neca J, Pencikova K, Palkova L, et al. Polar compounds dominate in vitro effects of sediment extracts. *Environmental science & technology*. 2011; 45:2384–2390. [PubMed: 21348526]
 56. MacDonald D, Ingersoll C, Smorong D, Lindskoog R, Sparks D, Smith J, et al. An assessment of injury to sediments and sediment-dwelling organisms in the Grand Calumet River and Indiana Harbor Area of Concern, USA. *Archives of environmental contamination and toxicology*. 2002; 43:141–155. [PubMed: 12115040]
 57. Mackenzie A, Brassell S, Eglinton G, Maxwell J. Chemical fossils: the geological fate of steroids. *Science*. 1982; 217:491. [PubMed: 17820518]
 58. Manan N, Raza M, Yuh YS, Theng LW, Zakaria MP. Distribution of petroleum hydrocarbons in aquaculture fish from selected locations in the Straits of Malacca, Malaysia. *World Applied Sciences Journal*. 2011; 14:14–21.
 59. MDH. Varney Pond: Stormwater Settling Pond Sediments. St. Paul, MN: 2011.
 60. Meyers PA, Ishiwatari R. Lacustrine organic geochemistry—an overview of indicators of organic matter sources and diagenesis in lake sediments. *Organic geochemistry*. 1993; 20:867–900.
 61. Neff, JM. Sources, Fates and Biological Effects. London, UK: Applied Science Publishers Ltd; 1979. Polycyclic Aromatic Hydrocarbons in The Aquatic Environment.
 62. Neff JM, Durell GS. Bioaccumulation of petroleum hydrocarbons in arctic amphipods in the oil development area of the Alaskan Beaufort Sea. *Integrated Environmental Assessment and Management*. 2012; 8:301–319. [PubMed: 22006590]
 63. Nevers MB, Whitman RL, Gerovac PJ. History and environmental setting of the Grand Calumet River. *Proceedings of the Indiana Academy of Science*. 2013; 108:3–10.
 64. Nisbet IC, LaGoy PK. Toxic equivalency factors (TEFs) for polycyclic aromatic hydrocarbons (PAHs). *Regulatory toxicology and pharmacology*. 1992; 16:290–300. [PubMed: 1293646]
 65. Ourisson G, Rohmer M. Hopanoids. 2. Biohopanoids: a novel class of bacterial lipids. *Accounts of Chemical Research*. 1992; 25:403–408.
 66. Ourisson G, Rohmer M, Poralla K. Prokaryotic hopanoids and other polyterpenoid sterol surrogates. *Annual Reviews in Microbiology*. 1987; 41:301–333.
 67. Ozaki N, Takemoto N, Kindaichi T. Nitro-PAHs and PAHs in atmospheric particulate matters and sea sediments in Hiroshima Bay Area, Japan. *Water, Air, and Soil Pollution*. 2010; 207:263–271.
 68. Perrini G, Tomasello M, Librando V, Minniti Z. Nitrated polycyclic aromatic hydrocarbons in the environment: formation, occurrences and analysis. *Annali di chimica*. 2005; 95:567–577. [PubMed: 16235790]
 69. Pistikopoulos P, Masclet P, Mouvier G. A receptor model adapted to reactive species: Polycyclic aromatic hydrocarbons; evaluation of source contributions in an open urban site—I. particle compounds. *Atmospheric Environment Part A General Topics*. 1990; 24:1189–1197.
 70. Prince RC, Elmendorf DL, Lute JR, Hsu CS, Haith CE, Senius JD, et al. 17. alpha.(H)-21. beta (H)-hopane as a conserved internal marker for estimating the biodegradation of crude oil. *Environmental science & technology*. 1994; 28:142–145. [PubMed: 22175843]
 71. Qu W, Xue B, Su C, Wang S. Evaluation of biogenic and anthropogenic inputs of aliphatic hydrocarbons to Lake Taihu sediments using biomarkers. *Hydrobiologia*. 2007; 581:89–95.
 72. Reisen F, Arey J. Atmospheric reactions influence seasonal PAH and nitro-PAH concentrations in the Los Angeles basin. *Environmental science & technology*. 2005; 39:64–73. [PubMed: 15667076]
 73. RIDEM. Rhode Island Air Toxics Guideline. State of Rhode Island Department of Environmental Management; Providence, RI: 2008.
 74. Sato T, Kato K, Ose Y, Nagase H, Ishikawa T. Nitroarenes in Suimon river sediment. *Mutation Research/Genetic Toxicology*. 1985; 157:135–143.
 75. Schantz MM, Porter BJ, Wise SA. Stability of Polycyclic Aromatic Hydrocarbons in Frozen Mussel Tissue. *Polycyclic Aromatic Compounds*. 2001; 19:253–262.

76. Schauer JJ, Kleeman MJ, Cass GR, Simoneit BR. Measurement of emissions from air pollution sources. 2. C1 through C30 organic compounds from medium duty diesel trucks. *Environmental Science & Technology*. 1999; 33:1578–1587.
77. Schauer JJ, Kleeman MJ, Cass GR, Simoneit BR. Measurement of emissions from air pollution sources. 3. C1–C29 organic compounds from fireplace combustion of wood. *Environmental Science & Technology*. 2001; 35:1716–1728. [PubMed: 11355184]
78. Schauer JJ, Kleeman MJ, Cass GR, Simoneit BR. Measurement of emissions from air pollution sources. 5. C1–C32 organic compounds from gasoline-powered motor vehicles. *Environmental science & technology*. 2002; 36:1169–1180. [PubMed: 11944666]
79. Schneider AR, Stapleton HM, Cornwell J, Baker JE. Recent declines in PAH, PCB, and toxaphene levels in the northern Great Lakes as determined from high resolution sediment cores. *Environmental science & technology*. 2001; 35:3809–3815. [PubMed: 11642437]
80. Simcik MF, Eisenreich SJ, Golden KA, Liu SP, Lipiatou E, Swackhamer DL, et al. Atmospheric loading of polycyclic aromatic hydrocarbons to Lake Michigan as recorded in the sediments. *Environmental science & technology*. 1996; 30:3039–3046.
81. Simcik MF, Eisenreich SJ, Lioy PJ. Source apportionment and source/sink relationships of PAHs in the coastal atmosphere of Chicago and Lake Michigan. *Atmospheric Environment*. 1999; 33:5071–5079.
82. Su MC, Christensen ER, Karls JF. Determination of PAH sources in dated sediments from Green Bay, Wisconsin, by a chemical mass balance model. *Environmental Pollution*. 1998; 99:411–419. [PubMed: 15093306]
83. Sun P, Backus S, Blanchard P, Hites RA. Annual variation of polycyclic aromatic hydrocarbon concentrations in precipitation collected near the Great Lakes. *Environmental science & technology*. 2006a; 40:696–701. [PubMed: 16509305]
84. Sun P, Blanchard P, Brice KA, Hites RA. Trends in polycyclic aromatic hydrocarbon concentrations in the Great Lakes atmosphere. *Environmental science & technology*. 2006b; 40:6221–6227. [PubMed: 17120545]
85. Szalinska E, Drouillard KG, Anderson EJ, Haffner GD. Factors influencing contaminant distribution in the Huron-Erie Corridor sediments. *Journal of Great Lakes Research*. 2011; 37:132–139.
86. Tang N, Hattori T, Taga R, Igarashi K, Yang X, Tamura K, et al. Polycyclic aromatic hydrocarbons and nitropolycyclic aromatic hydrocarbons in urban air particulates and their relationship to emission sources in the Pan–Japan Sea countries. *Atmospheric Environment*. 2005; 39:5817–5826.
87. Thurston GD, Spengler JD. A quantitative assessment of source contributions to inhalable particulate matter pollution in metropolitan Boston. *Atmospheric Environment (1967)*. 1985; 19:9–25.
88. Tokiwa H, Nakagawa R, Morita K, Ohnishi Y. Mutagenicity of nitro derivatives induced by exposure of aromatic compounds to nitrogen dioxide. *Mutation Research/Environmental Mutagenesis and Related Subjects*. 1981; 85:195–205.
89. USEPA. Field Sampling Guidance Document #1215: Sediment Sampling. Rev. 1. U.S. EPA Region 9 Laboratory; Richmond, CA: 1999.
90. van Dongen BE, Rowland HA, Gault AG, Poly DA, Bryant C, Pancost RD. Hopane, sterane and *n*-alkane distributions in shallow sediments hosting high arsenic groundwaters in Cambodia. *Applied Geochemistry*. 2008; 23:3047–3058.
91. Van Metre P.; Mahler, BJ.; Burbank, TL.; Wilson, JT. Collection and Analysis of Samples for Polycyclic Aromatic Hydrocarbons in Dust and Other Solids Related to Sealed and Unsealed Pavement from 10 Cities Across the United States, 2005–07. US Department of the Interior, US Geological Survey; 2008.
92. Van Metre PC, Mahler BJ. Contribution of PAHs from coal–tar pavement sealcoat and other sources to 40 US lakes. *Science of the total environment*. 2010; 409:334–344. [PubMed: 21112613]

93. Van Metre PC, Majewski MS, Mahler BJ, Foreman WT, Braun CL, Wilson JT, et al. Volatilization of polycyclic aromatic hydrocarbons from coal-tar-sealed pavement. *Chemosphere*. 2012; 88:1–7. [PubMed: 22289152]
94. Wang Q, Li Y, Wang Y. Optimizing the weight loss-on-ignition methodology to quantify organic and carbonate carbon of sediments from diverse sources. *Environmental monitoring and assessment*. 2011a; 174:241–257. [PubMed: 20424912]
95. Wang XC, Sun S, Ma HQ, Liu Y. Sources and distribution of aliphatic and polyaromatic hydrocarbons in sediments of Jiaozhou Bay, Qingdao, China. *Marine Pollution Bulletin*. 2006; 52:129–138. [PubMed: 16194554]
96. Wang Z, Yang C, Yang Z, Sun J, Hollebne B, Brown C, et al. Forensic fingerprinting and source identification of the 2009 Sarnia (Ontario) oil spill. *Journal of Environmental Monitoring*. 2011b; 13:3004–3017. [PubMed: 21956546]
97. WDNR. Consensus-Based Sediment Quality Guidelines: Recommendations for Use & Application. Wisconsin Department of Natural Resources; Madison, WI: 2003.
98. Xiong Y, Wu F, Fang J, Wang L, Li Y, Liao H. Organic geochemical record of environmental changes in Lake Dianchi, China. *Journal of Paleolimnology*. 2010; 44:217–231.
99. Yaffe D, Cohen Y, Arey J, Grosovsky AJ. Multimedia analysis of PAHs and nitro-PAH daughter products in the Los Angeles basin. *Risk Analysis*. 2001; 21:275–294. [PubMed: 11414537]
100. Yunker MB, Macdonald RW, Vingarzan R, Mitchell RH, Goyette D, Sylvestre S. PAHs in the Fraser River basin: a critical appraisal of PAH ratios as indicators of PAH source and composition. *Organic Geochemistry*. 2002; 33:489–515.
101. Zhang X, Christensen ER, Gin MF. Polycyclic aromatic hydrocarbons in dated sediments from Green Bay and Lake Michigan. *Estuaries*. 1993; 16:638–652.
102. Zhang Y, Guo CS, Xu J, Tian YZ, Shi GL, Feng YC. Potential source contributions and risk assessment of PAHs in sediments from Taihu Lake, China: comparison of three receptor models. *Water research*. 2012; 46:3065–3073. [PubMed: 22459329]

Highlights

- 37 SVOCs are measured in 24 surface sediment samples from southern Lake Michigan.
- PAH levels have declined by three to four folds since the 1980s.
- Carcinogenic nitro-PAHs are detected and are widely distributed.
- OC-adjusted SVOC concentrations in open water sediments show gradients from sources.
- The major sources of PAHs are vehicle exhaust, coal combustion and coal-tar sealcoat.



Figure 1. Lake Michigan sampling sites. The green shaded area surrounding the lake indicates the drainage area.

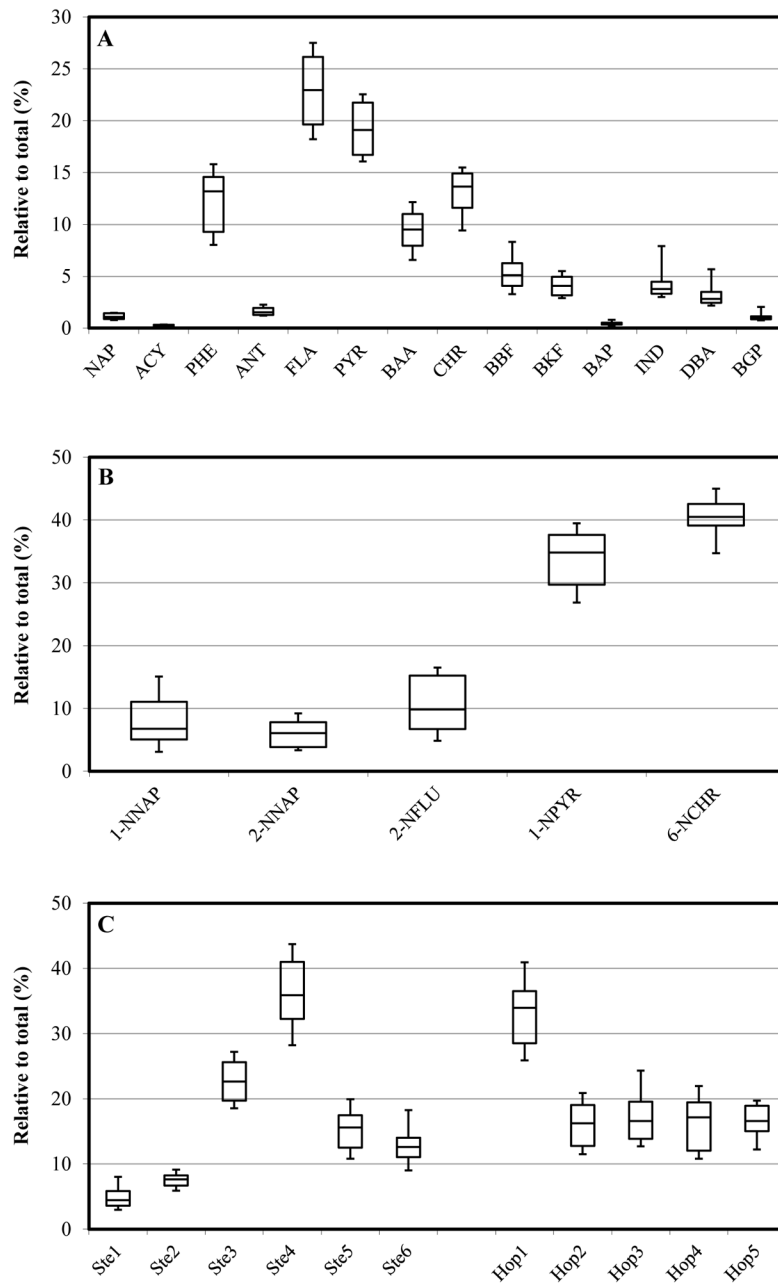


Figure 2. Boxplots showing the concentrations of individual (A) PAHs; (B) NPAHs; and (C) biomarkers that are normalized to the corresponding total concentrations. Boxplots show 10th, 25th, 50th, 75th and 90th percentiles.

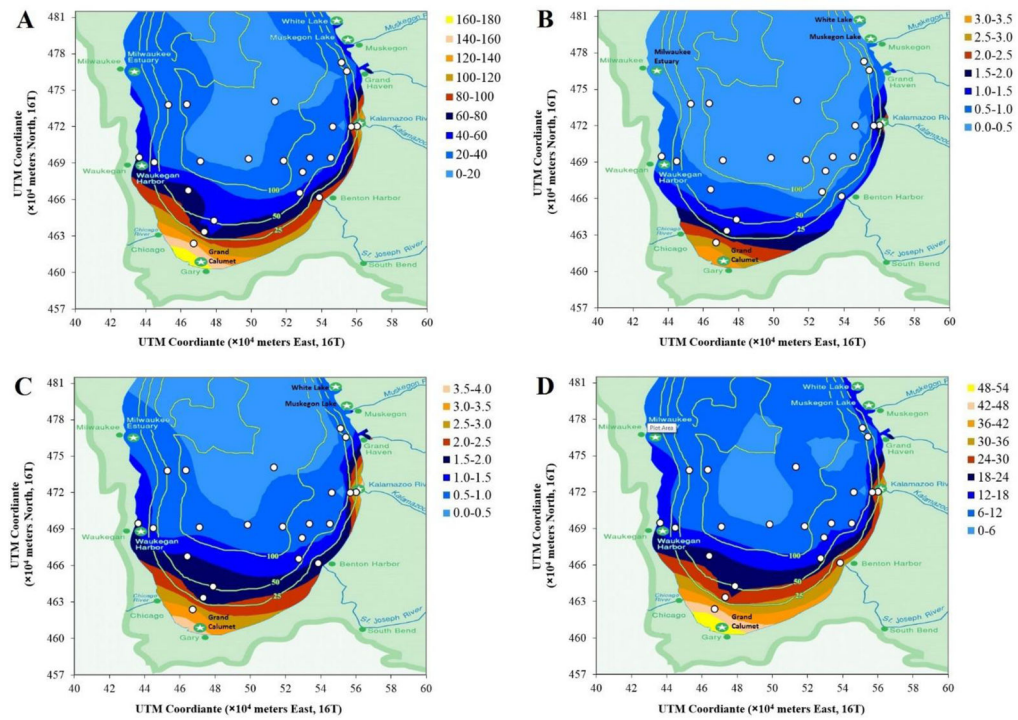


Figure 3. Concentration maps of OC-adjusted concentrations of (A) ΣPAH_{14} ; (B) ΣNPAH_5 ; (C) $\Sigma\text{Sterane}_6$; and (D) ΣHopane_5 . Units are $\mu\text{g/g OC}$. White dots indicate sediment sampling sites in this study. Graph axes show Universal Transverse Mercator coordinate system.

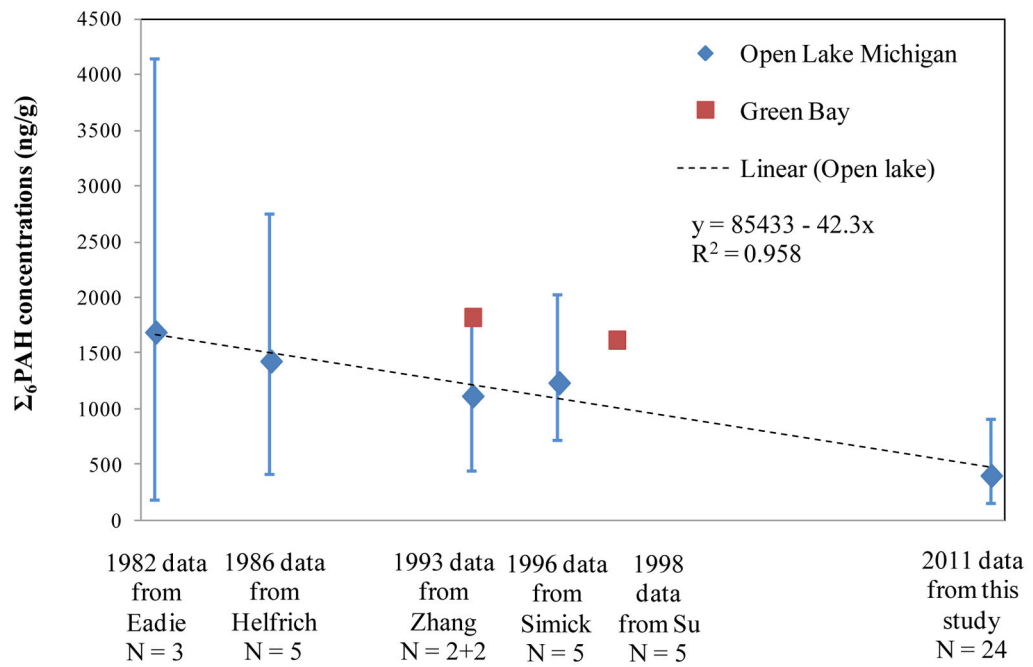


Figure 4. Trend of $\Sigma_6\text{PAH}$ concentrations in Lake Michigan sediments (showing mean, maximum and minimum of observations, plus regression line). $\Sigma\text{PAH}_6 = 85433 - 42.3x$, where x is time (year).

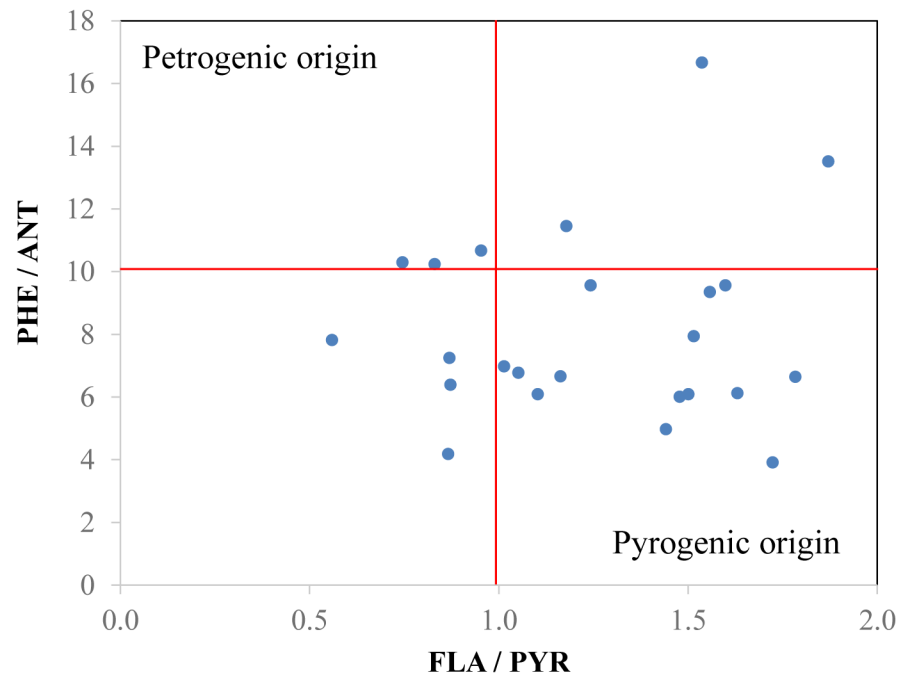


Figure 5. Plot of PHE / ANT ratios against FLA / PYR ratios for all samples.

Table 1

List of target compounds, and summary of study measurements.

Group	Compound	Abbrev.	CAS #	MW (g/mol)	# of rings	MDL (ng/g dw)	Study measurements (ng/g dry sediment)				
							Mean	Std	Min	Max	Detection freq. (%) (N = 24)
	Naphthalene	NAP	91-20-3	128	2	0.03	6.2	2.8	2.5	12.7	100
	Acenaphthylene	ACY	208-96-8	152	3	0.07	1.4	0.7	0.7	3.9	100
	Acenaphthene	ACT	83-32-9	154	3	0.07	-	-	-	-	0
	Fluorene	FLU	86-73-7	166	3	0.10	0.22	0.30	ND	1.1	37
	Phenanthrene	PHE	85-01-8	178	3	0.07	70.4	36.3	29.1	179.1	100
	Anthracene	ANT	120-12-7	178	3	0.05	9.1	4.4	3.8	18.7	100
	Fluoranthene	FLA	206-44-0	202	4	0.10	134.1	84.2	47.3	385.2	100
	Pyrene	PYR	129-00-0	202	4	0.05	110.3	57.7	25.3	236.3	100
PAHs	Benz[a]anthracene	BAA	56-55-3	228	4	0.05	55.8	35.3	12.0	167.4	100
	Chrysene	CHR	218-01-9	228	4	0.08	75.9	40.4	19.3	175.3	100
	Benzo[b]fluoranthene	BBF	205-99-2	252	5	0.13	28.5	13.2	13.2	71.9	100
	Benzo[k]fluoranthene	BKF	207-08-9	252	5	0.14	22.5	9.5	10.4	44.2	100
	Benzo[a]pyrene	BAP	50-32-8	252	5	0.06	2.7	2.0	1.0	10.2	100
	Dibenzo[a,h]anthracene	DBA	53-70-3	278	5	0.53	24.9	17.9	7.8	95.4	100
	Indeno[1,2,3-cd]pyrene	IND	193-39-5	276	6	0.38	18.2	13.5	5.9	74.1	100
	Benzo[g,h,i]perylene	BGP	191-24-2	276	6	0.02	6.7	5.2	2.3	27.5	100
	1-Nitronaphthalene	1-NNAP	86-57-7	173	2	0.07	0.61	0.39	0.19	1.69	100
	2-Nitronaphthalene	2-NNAP	581-89-5	173	2	0.09	0.52	0.42	0.13	2.15	100
	2-Nitrobiphenyl	2-NBPL	86-00-0	199	2	0.07	-	-	-	-	0
	3-Nitrobiphenyl	3-NBPL	2113-58-8	199	2	0.06	-	-	-	-	0
	4-Nitrobiphenyl	4-NBPL	92-93-3	199	2	0.27	-	-	-	-	0
NPAHs	5-Nitroacenaphthene	5-NACT	602-87-9	199	3	0.02	-	-	-	-	0
	2-Nitrofluorene	2-NFLU	607-57-8	211	3	0.11	0.83	0.55	0.22	2.64	100
	9-Nitroanthracene	9-NAANT	602-60-8	223	3	0.02	-	-	-	-	0
	9-Nitrophenanthrene	9-NPHE	954-46-1	223	3	0.01	-	-	-	-	0
	1-Nitropyrene	1-NPYR	5522-43-0	247	4	0.01	2.67	1.41	0.85	6.44	100
	6-Nitrochrysene	6-NCHR	7496-02-8	273	4	0.06	3.22	1.67	1.15	8.09	100

Group	Compound	Abbrev.	CAS #	MW (g/mol)	# of rings	MDL (ng/g dw)	Study measurements (ng/g dry sediment)				Detection freq. (%) (N = 24)
							Mean	Std	Min	Max	
Steranes	20S-5 α (h), 14 α (h), 17 α (h)-Cholestane	Ste1	41083-75-4	373	4	0.02	0.7	0.5	0.2	1.7	100
	20R-5 α (h), 14 α (h), 17 α (h)-Cholestane	Ste2	481-21-0	373	4	0.03	1.1	0.5	0.4	2.8	100
	20R-5 α (h), 14 β (h), 17 β (h)-Cholestane	Ste3	69483-47-2	373	4	0.02	3.4	1.9	1.3	8.4	100
	20R-5 α (h), 14 β (h), 17 β (h)-24-Methylcholestane	Ste4	71117-90-3	387	4	0.03	5.5	3.6	1.7	15.2	100
	20R-5 α (h), 14 α (h), 17 α (h)-24-Ethylcholestane	Ste5	62446-14-4	401	4	0.02	2.2	1.3	1.0	5.7	100
	20R-5 α (h), 14 β (h), 17 β (h)-24-Ethylcholestane	Ste6	71117-92-5	401	4	0.03	1.9	1.2	0.7	5.2	100
Hopanes	17 α (h),21 β (h)-Hopane	Hop1	471-62-5	413	5	0.02	64.5	34.3	28.6	160.8	100
	17 α (h)-22,29,30-Trisnorhopane	Hop2	53584-59-1	371	5	0.04	30.9	15.9	11.7	70.9	100
	17 α (h),21 β (h)-30-Norhopane	Hop3	53584-60-4	399	5	0.04	33.3	18.9	12.5	92.4	100
	22R-17 α (h),21 β (h)-Homohopane	Hop4	60305-22-8	427	5	0.02	31.0	16.5	9.9	79.6	100
	22S-17 α (h),21 β (h)-Homohopane	Hop5	60305-23-9	427	5	0.02	31.5	17.1	15.9	76.3	100

MW: molecular weight. MDL: instrument detection limit. Std: standard deviation. ND: not detected.

Table 2
Diagnostic ratios used to identify possible sources of target SVOCs in Lake Michigan sediments

Ratio	Definition	Interpretation	Reason	Reference
PAHs				
PHE/ANT	PHE/ANT	<10: pyrogenic; >10: petrogenic.	Difference in thermodynamic stability.	Budzinski et al., 1997
FLA/PYR	FLA/PYR	<1: petrogenic; >1: pyrogenic.	Difference in thermodynamic stability.	Budzinski et al., 1997
BAA/CHR	BAA/CHR	Decreases from urban to remote sites.	BAA is more susceptible to photo-oxidation than CHR.	Gschwend et al., 1981
ANT/178	ANT/(ANT+PHE)	<0.1: petroleum; >0.1: combustion.	Difference in thermodynamic stability.	Yunker et al., 2002
FLA/202	FLA/(FLA+PYR)	<0.4: petroleum; 0.4–0.5: liquid fossil fuel combustion; >0.5: grass, wood or coal combustion.	Difference in thermodynamic stability.	Yunker et al., 2002
BAA/228	BAA/(BAA+CHR)	<0.2: petroleum; >0.35: combustion.	Difference in thermodynamic stability.	Yunker et al., 2002
IND/276	IND/(IND+BGP)	<0.2: petroleum; 0.2–0.5: liquid fossil fuel combustion; >0.5: grass, wood or coal combustion.	Difference in thermodynamic stability.	Yunker et al., 2002
$\Sigma^{LPAHs}/\Sigma^{HPAHs}$	sum of 3-ring PAHs / sum of > 3-ring PAHs	<1: petrogenic; >1: pyrogenic.	More larger PAHs are formed during combustion.	Wang et al., 2006
NPAHs				
1-NPYR/PYR	1-nitropyrene/pyrene	0.36: diesel engines; 0.001: coal combustion.	Formation of NPAHs increase with increasing temperature.	Tang et al., 2005
Hopanes and steranes				
$C_{31-22S}/(22S+22R)$	$22S-17\alpha(h),21\beta(h)\text{-homohopane}/[22S-17\alpha(h),21\beta(h)\text{-homohopane}+22R-17\alpha(h),21\beta(h)\text{-homohopane}]$	0.6 indicates full maturity (petroleum); >0.5: petrogenic dominates; <0.5: biogenic dominates.	Thermal maturity indicator.	Hosettler et al., 1992

Table 3

Lake Michigan sampling sites, physical data and SVOC concentrations

Site	Latitude (°N)	Longitude (°W)	Water depth (m)	Distance from shore (km)	AOC/industrial/urban areas (km)	Distance to nearest AOC/industrial/urban areas (km)	Sediment type	Moisture content (%)	OC (%)	Σ_{15} PAH (ng/g dry)	Σ_{11} NPAH (ng/g dry)	Σ_6 Sterane (ng/g dry)	Σ_5 Hopane (ng/g dry)
A-1	42.108	86.533	16	3.4	3.8	3.8	sand	8.4	0.6	496.9	5.13	9.7	174.4
B-2	42.400	86.450	52	13.3	34.2	34.2	silt	60.1	3.5	802.8	10.52	18.1	300.2
B-3	42.400	86.592	64	24.3	42.1	42.1	silt	59.2	2.3	831.6	8.20	20.6	256.1
B-4	42.392	87.017	124	53.9	53.5	53.5	silt over loam	60.0	3.6	513.0	9.60	17.7	196.2
B-5	42.375	87.350	108	38.0	38.9	38.9	silt over loam	49.3	2.7	508.6	9.13	21.3	207.4
B-6	42.375	87.500	84	25.6	26.6	26.6	silt over loam	40.6	4.7*	327.3	6.59	11.4	138.9
B-7	42.367	87.667	45	12.0	12.8	12.8	silty sand	33.5	0.9	312.8	4.89	6.4	103.1
C-5	42.817	86.833	136	50.8	53.1	53.1	silt	64.0	4.6	860.2	17.02	20.8	323.0
C-6	42.795	87.447	105	25.4	44.6	44.6	silt over sandy loam	39.1	1.6	421.8	5.23	8.8	113.6
C-7	42.792	87.575	60	15.0	36.8	36.8	silt over sandy loam	47.8	2.0	609.5	8.50	15.6	221.2
EG-14	42.378	86.775	98	36.7	37.7	37.7	silt	62.0	4.4	1290.8	14.48	36.0	355.0
EG-18	42.293	86.643	60	22.2	23.6	23.6	silt	47.4	2.3	588.5	6.18	19.5	255.3
H-15	42.158	87.433	60	22.9	34.1	34.1	silty sand	28.4	0.5	332.6	2.91	7.8	102.3
H-22	42.139	86.664	48	14.6	14.8	14.8	silt	60.1	2.1	903.1	6.52	24.0	332.6
H-28	42.630	86.265	22	2.9	5.2	5.2	medium to coarse sand	18.2	0.3	347.4	5.64	10.0	98.7
H-29	42.630	86.306	32	6.3	8.3	8.3	silt	39.7	1.8	364.3	6.85	7.4	114.0
H-30	42.630	86.433	70	16.7	18.6	18.6	silt	66.1	4.0	1234.5	18.59	33.3	351.1
H-31	43.041	86.333	45	6.9	21.4	21.4	silt, some sand	55.6	3.0	588.9	8.90	15.1	186.0
H-8	42.399	87.771	19	2.6	6.0	6.0	silt with some clay	28.9	0.8	451.2	5.73	11.2	116.4
S-2	41.765	87.391	13	8.5	11.7	11.7	fine sand	20.6	0.3	398.1	7.81	8.8	125.8
S-3	41.850	87.320	25	19.4	22.7	22.7	silty sand	21.6	0.5	212.8	5.01	6.2	97.7
S-4	41.935	87.252	40	30.4	33.7	33.7	silty sand	23.8	0.5	315.8	6.85	9.5	127.8
V-1	41.697	87.013	17	1.6	35.9	35.9	clay, some sand	18.3	4.6*	329.2	3.74	6.8	111.3
X-1	43.103	86.367	45	7.9	14.7	14.7	silt	42.2	1.7	564.1	6.76	10.4	181.1
Mean								41.5	2.2	566.9	8.0	14.8	191.2
Std								17.4	1.5	286.1	3.9	8.2	88.4
Min								8.4	0.3	212.8	2.9	6.2	97.7

Site	Latitude (°N)	Longitude (°W)	Water depth (m)	Distance from shore (km)	Distance to nearest AOC/industrial/urban areas (km)	Sediment type	Moisture content (%)	OC (%)	Σ_{13} PAH (ng/g dry)	Σ_{11} NPAH (ng/g dry)	Σ_6 Sterane (ng/g dry)	Σ_5 Hopane (ng/g dry)
Max							66.1	4.7	1290.8	18.6	36.0	355.0

OC: organic carbon. Std: standard deviation.

OC values marked with an asterisk were not used in regression analyses (see Section 2.4).

Table 4

SVOC diagnostic ratio results (organized based on distance from shore)

Site	Distance from shore (km)	Distance to nearest AOC/ industrial/ urban areas (km)	BAA/CHR	PHE/ANT	FLA/PYR	ANT/178	FLA/202	BAA/228	IND/276	ΣLPAHs/ΣHPAHs	I-NPYR/PYR	C ₃₁ -22S/(22S+22R)
V-1	1.6	35.9	0.69	7.9	1.5	0.11	0.60	0.41	0.77	0.19	0.016	0.62
H-8	2.6	6	0.70	6.1	1.5	0.14	0.60	0.41	0.82	0.15	0.025	0.52
H-28	2.9	5.2	0.73	3.9	1.7	0.20	0.63	0.42	0.79	0.14	0.030	0.50
A-1	3.4	3.8	0.71	7.0	1.0	0.13	0.50	0.42	0.78	0.19	0.014	0.51
H-29	6.3	8.3	0.67	6.7	1.2	0.13	0.54	0.40	0.81	0.13	0.034	0.46
H-31	6.9	21.4	0.68	6.6	1.8	0.13	0.64	0.40	0.83	0.14	0.027	0.47
X-1	7.9	14.7	0.68	11.5	1.2	0.08	0.54	0.40	0.78	0.21	0.018	0.47
S-2	8.5	11.7	0.55	6.1	1.1	0.14	0.52	0.35	0.80	0.22	0.036	0.58
B-7	12.0	12.8	0.72	10.2	0.8	0.09	0.45	0.42	0.83	0.19	0.028	0.44
B-2	13.3	34.2	0.75	10.7	1.0	0.09	0.49	0.43	0.77	0.20	0.021	0.51
H-22	14.6	14.8	0.72	6.0	1.5	0.14	0.60	0.42	0.81	0.16	0.010	0.64
C-7	15.0	36.8	0.69	9.6	1.2	0.09	0.55	0.41	0.82	0.20	0.027	0.42
H-30	16.7	18.6	0.96	6.1	1.6	0.14	0.62	0.49	0.80	0.11	0.027	0.43
S-3	19.4	22.7	0.62	13.5	1.9	0.07	0.65	0.38	0.77	0.43	0.080	0.39
EG-18	22.2	23.6	0.85	6.8	1.1	0.13	0.51	0.46	0.81	0.24	0.017	0.65
H-15	22.9	34.1	0.73	9.4	1.6	0.10	0.61	0.42	0.81	0.24	0.018	0.64
B-3	24.3	42.1	0.75	10.3	0.7	0.09	0.43	0.43	0.77	0.21	0.011	0.37
C-6	25.4	44.6	0.75	7.8	0.6	0.11	0.36	0.43	0.80	0.11	0.017	0.47
B-6	25.6	26.6	0.73	7.2	0.9	0.12	0.47	0.42	0.77	0.14	0.034	0.47
S-4	30.4	33.7	0.95	5.0	1.4	0.17	0.59	0.49	0.78	0.23	0.044	0.54
EG-14	36.7	37.7	0.71	9.6	1.6	0.09	0.62	0.41	0.78	0.20	0.021	0.49
B-5	38.0	38.9	0.55	6.4	0.9	0.14	0.47	0.36	0.77	0.20	0.024	0.49
C-5	50.8	53.1	0.77	4.2	0.9	0.19	0.46	0.44	0.78	0.13	0.032	0.60
B-4	53.9	53.5	0.57	16.7	1.5	0.06	0.61	0.36	0.77	0.30	0.046	0.43
Mean			0.72	8.1	1.3	0.12	0.54	0.42	0.79	0.19	0.027	0.51
Std			0.1	3.0	0.4	0.0	0.1	0.0	0.0	0.1	0.0	0.1

Site	Distance from shore (km)	Distance to nearest AOC/ industrial/ urban areas (km)	BAA/CHR	PHE/ANT	FLA/PYR	ANT/178	FLA/202	BAA/228	IND/276	Σ LPAHs/ Σ HPAHs	1-NPYR/PYR	C _{31r} -22S/(22S+22R)
Min			0.55	3.9	0.6	0.06	0.36	0.35	0.77	0.11	0.010	0.37
Max			0.96	16.7	1.9	0.20	0.65	0.49	0.83	0.43	0.080	0.65